From 3D Dosimetry to CT and Radiography imaging using Scintillator Detectors

Sam Beddar, Professor

Director of Clinical Research

The University of Texas MD Anderson Cancer Center &

The University of Texas Graduate School of Biomedical Sciences

Disclosures

- The University of Texas MD Anderson Cancer Center & l'Université Laval have two license agreements with Standard Imaging.
- SB & LB had an NIH/NCI SBIR Phase I and Phase II grants (R43 and R42) with Standard Imaging.
- LB & SB had Sponsored Research Agreement with Standard Imaging.
- SB had phase I, II, III Sponsored Research Agreements with Radiadyne, LLC.
- The Danish Cancer Society and Novo Nordisk Foundation grants in collaboration with the Aarhus Group (Kari Tanderup and Jacob Johansen

Outline

- **Introduction**
  - Basic properties of PSDs
- **Quality Assurance & Applications**
  - Exradin W1 and W2 scintillators
  - Small field dosimetry
  - *In vivo* dosimetry
- **Volumetric (3D) Dosimetry**
- **Radiography Imaging**

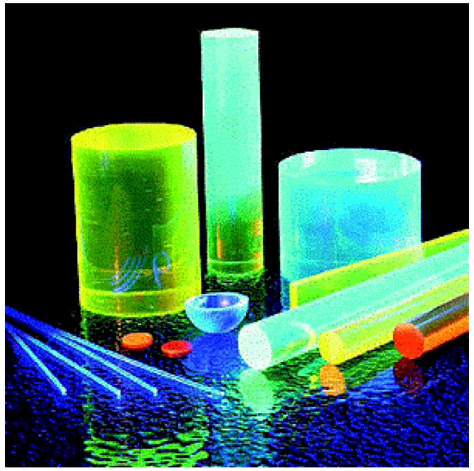

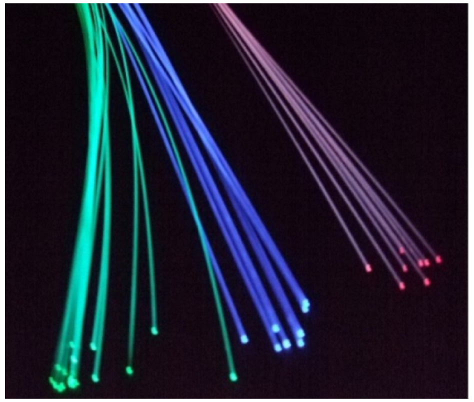

What is a PSD?

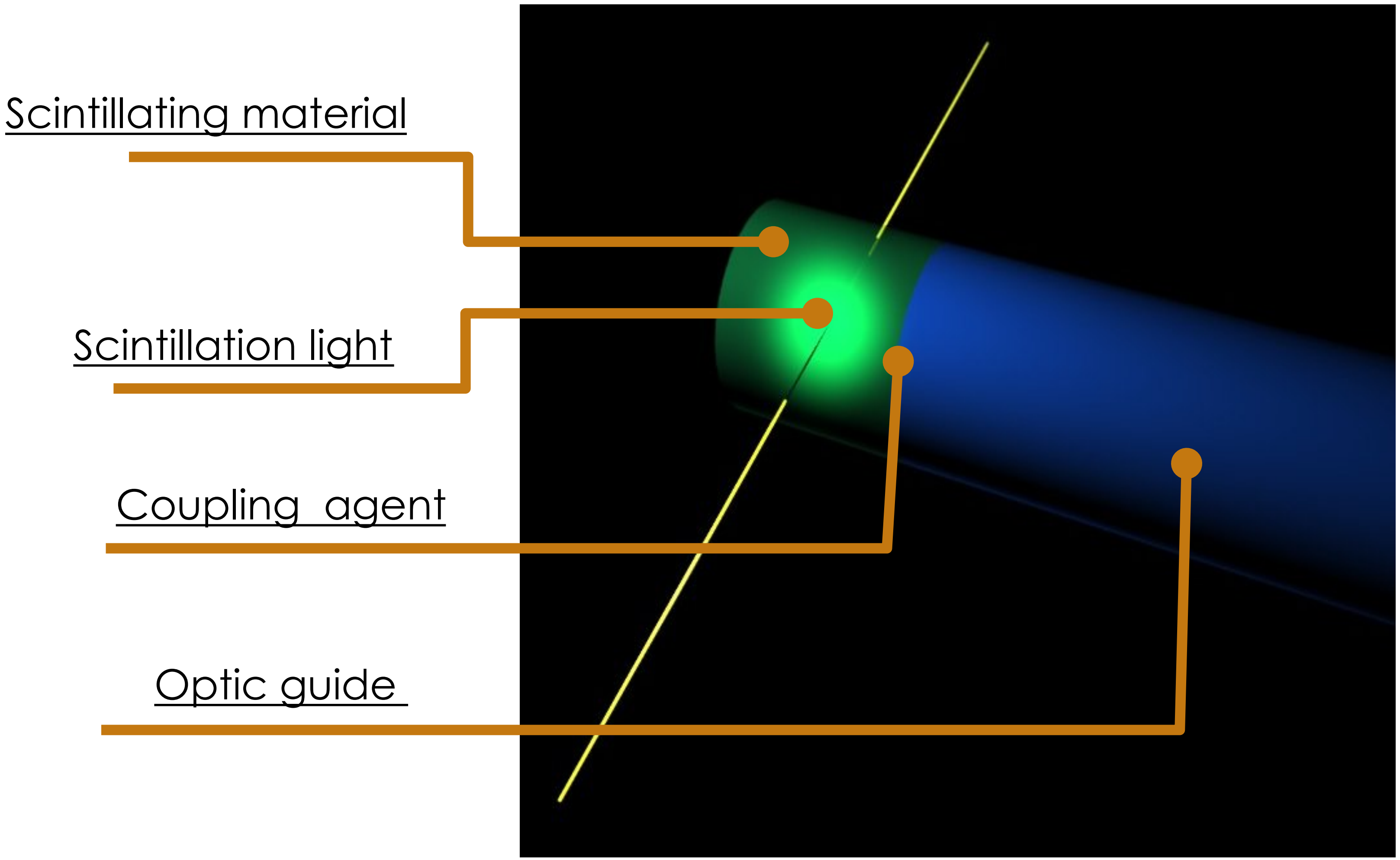
Scintillating material
Scintillation light
Coupling agent
Optic guide

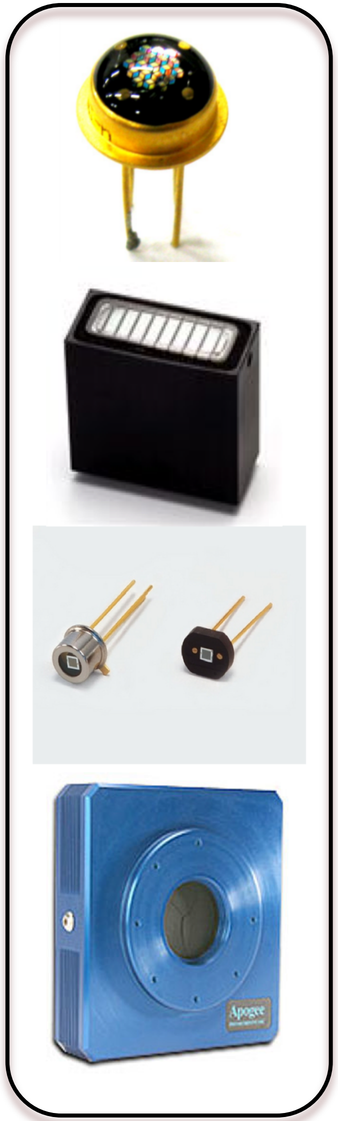

Water Equivalence

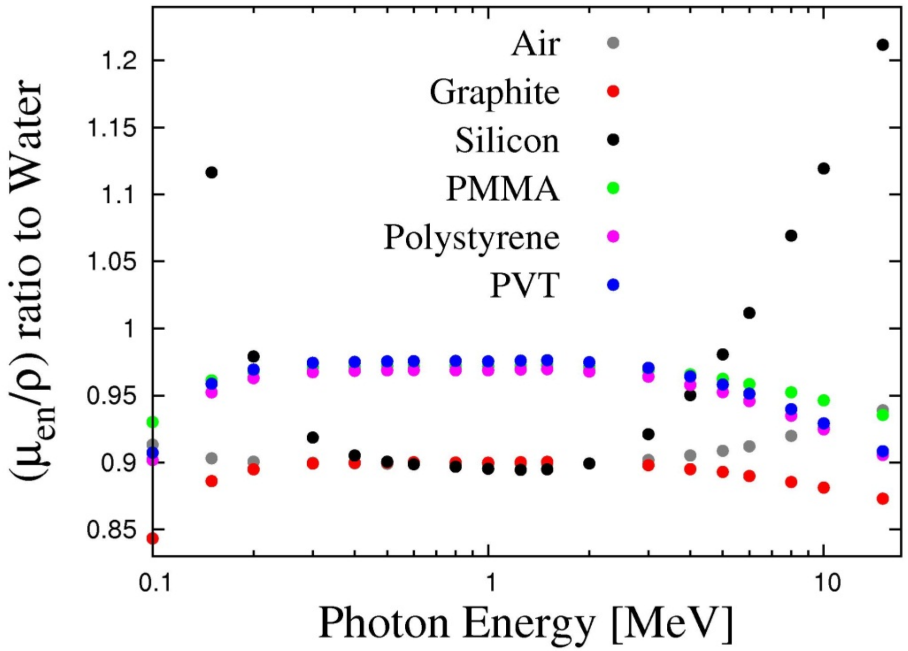

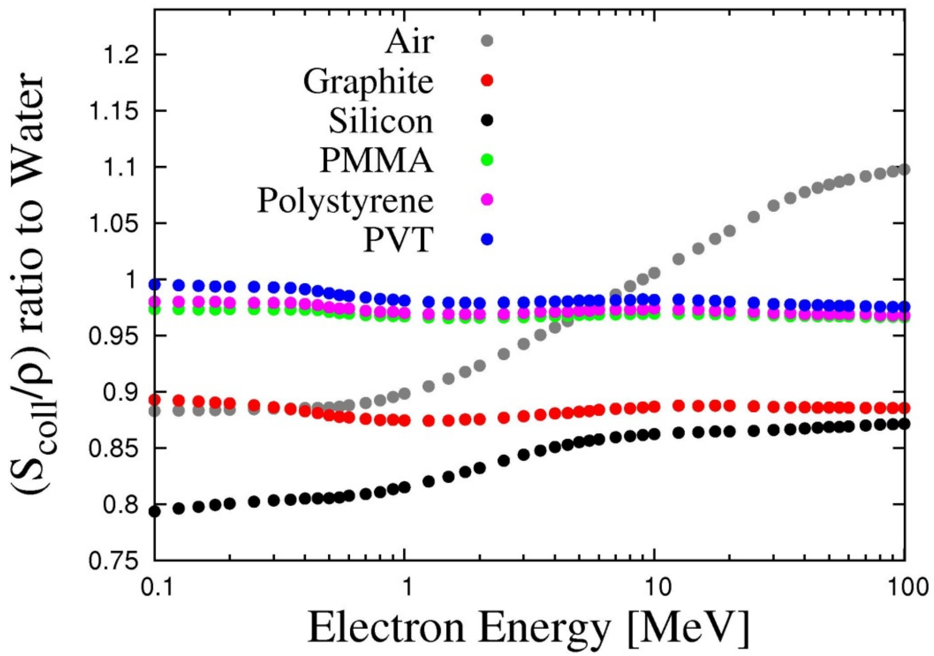

Data from NIST

Properties

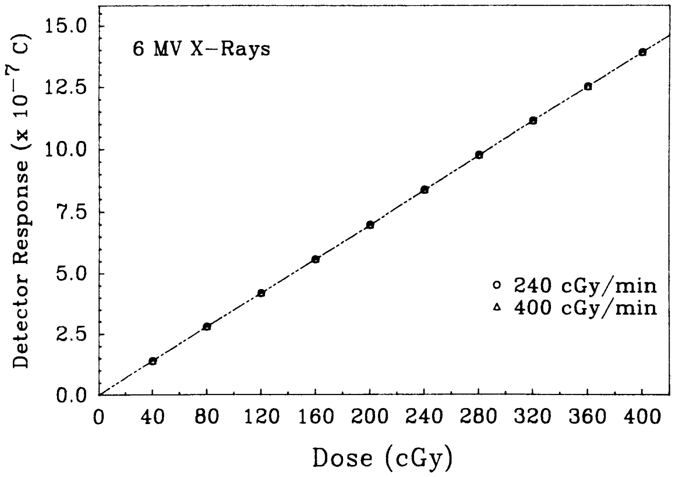

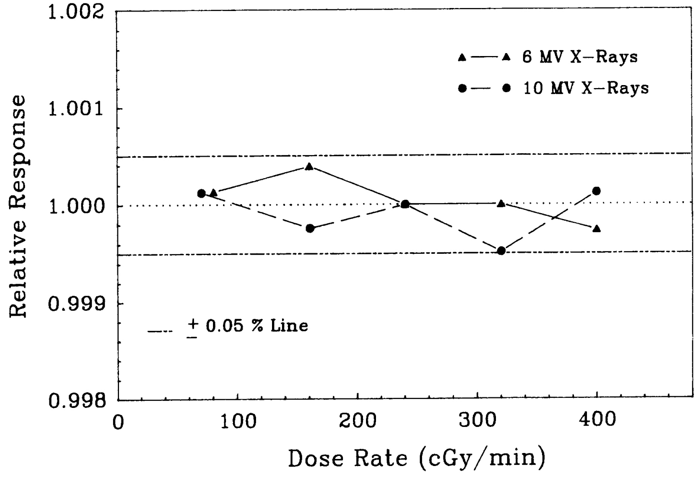

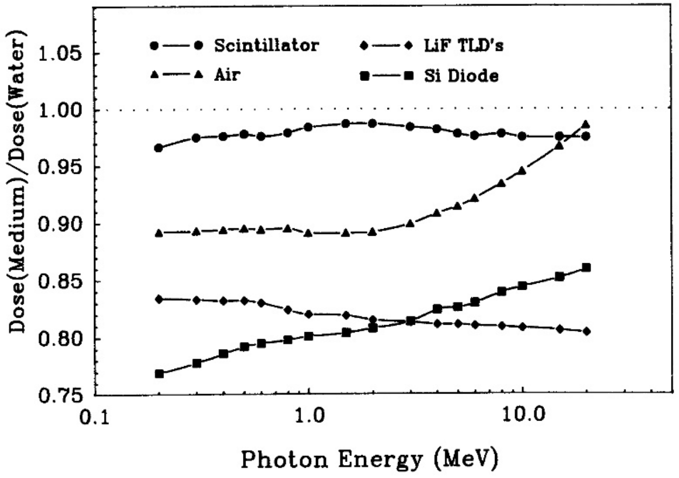

$$\frac{\overline{D}_{sci}}{\overline{D}_{med}} = 0.980 \pm 0.005$$

Beddar A S, Mackie T R, Attix F H. **Water-equivalent plastic scintillation detectors for high-energy beam dosimetry: I. Physical characteristics and theoretical considerations.** *Phys Med Biol* 37: 1883-1900, 1992.

Advantages of Plastic Scintillators

- ✓ Linear response to dose
- ✓ Dose rate independence
- ✓ Energy independence
- ✓ Particle type independence for photons and electrons
- ✓ Insensitive to RF fields
- ✓ Real-time readout
- ✓ Spatial resolution
- ✓ Fast (Real-time) response

Quality Assurance
Field Characterization
&
Small Field Dosimetry

A Daily QA Detector Device

- Rugged, simple to construct & cost effective
- Good stability and reproducibility
- Independent of temperature and pressure
- No high-voltage bias
- Remote operation and reset & Easily used by trained technical staff

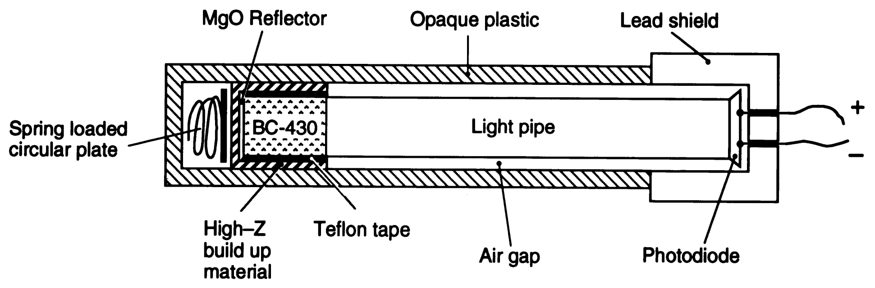

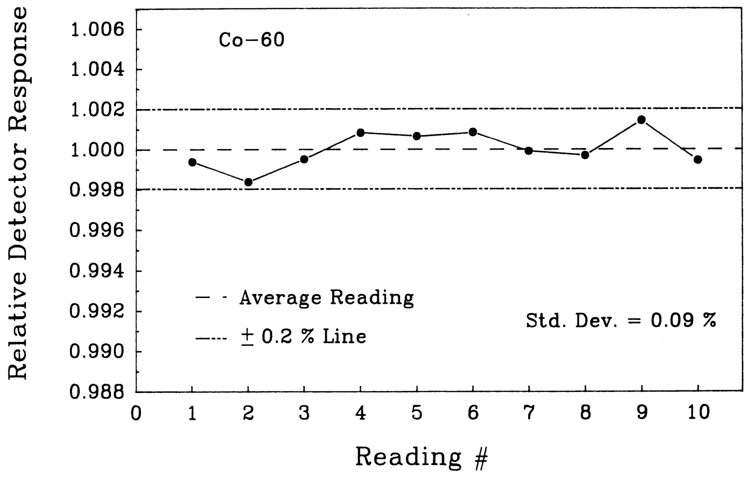

Beddar S, "**A new scintillator detector system for the quality assurance of ^{60}Co and high-energy therapy machines**". *Phys Med Biol 39: 253–263, 1994.*

Exradin W1 Scintillator

- Detector:
  - < 2.3 mm^3 sensitive volume (1)
  - Clear optical fiber for transport (2)

- Photodetector (3)
  - Two channels
    - Chromatic stem effect removal
  - Stay in the vault, <u>but shielded</u>

- Two channels electrometer with dedicated software (4)

4

Exradin W2 Scintillator

- AAPM/IAEA TRS 483 states the scintillator is the only detector with a kQ of 1.000, making the W2 the ideal SRS detector
- All corrections are built in
- Water equivalent
- Inherently waterproof
- Can be used for both water scanning and point dosimetry
- User replaceable fiber, includes both 1x1 mm and 1x3 mm

- No dose rate, temperature, or energy dependencies
- The W2 system features Čerenkov corrected measurement signals that can be converted to a proportional analog output, which can be read by any electrometer. This allows the W2 system to be connected to a water phantom system for scanning.

The Exradin W2 Scintillator is the ideal small field measurement tool

overcoming dependencies present in conventional detectors

SMALL FIELDS AND RADIOSURGERY (2001)

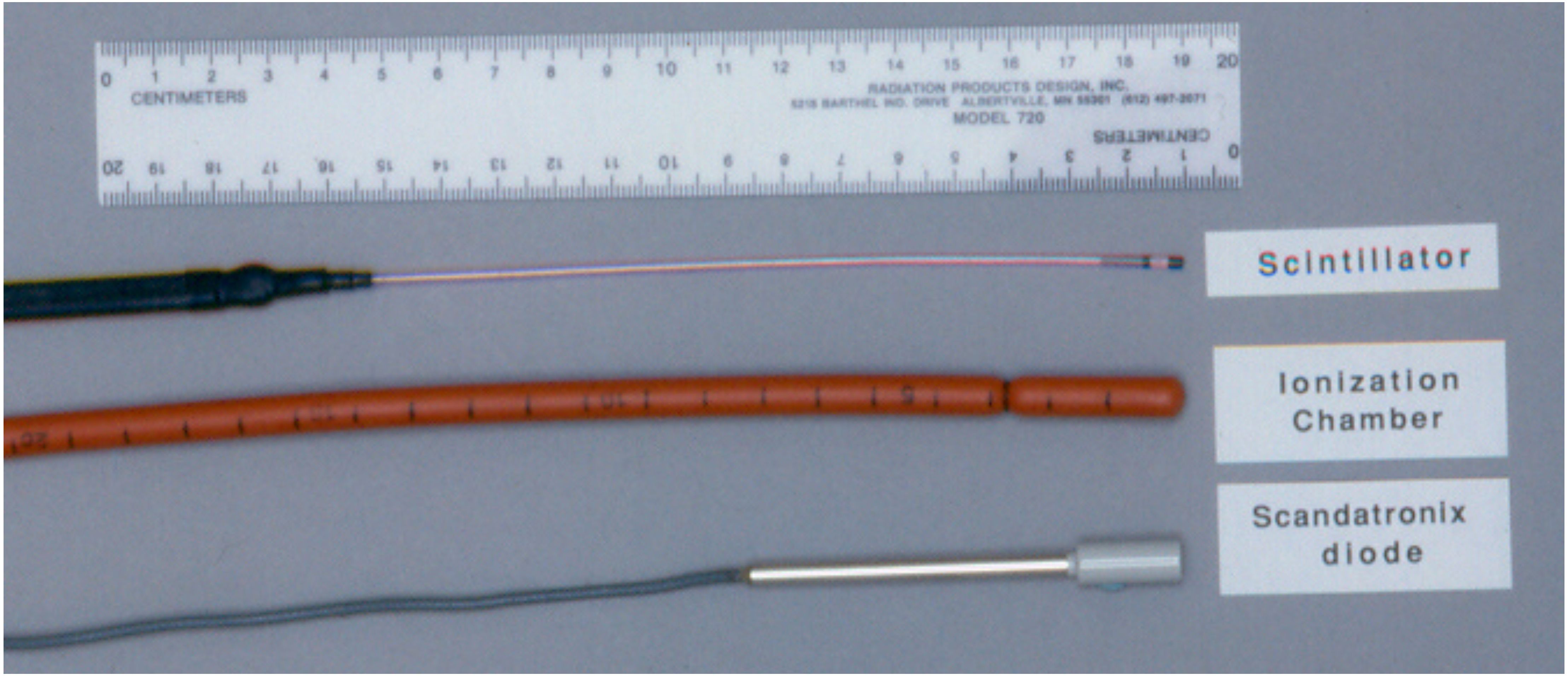

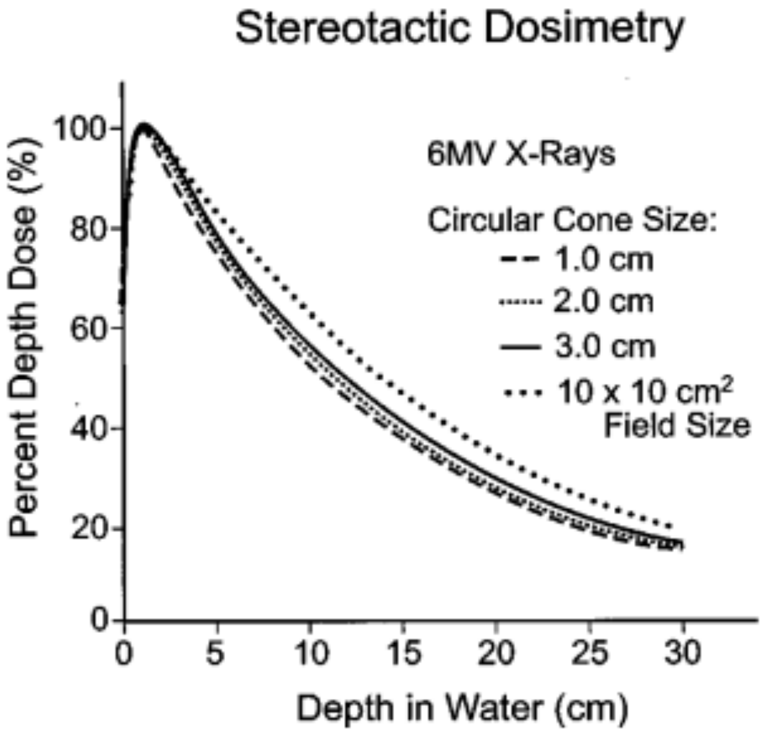

Fig. 3. Absorbed dose as a function of depth in water, normalized to depth d_{max} for the 10-, 20-, and 30-mm cone using the scintillator detector. The percent depth dose for the 10×10 cm^2 reference field size is also shown.

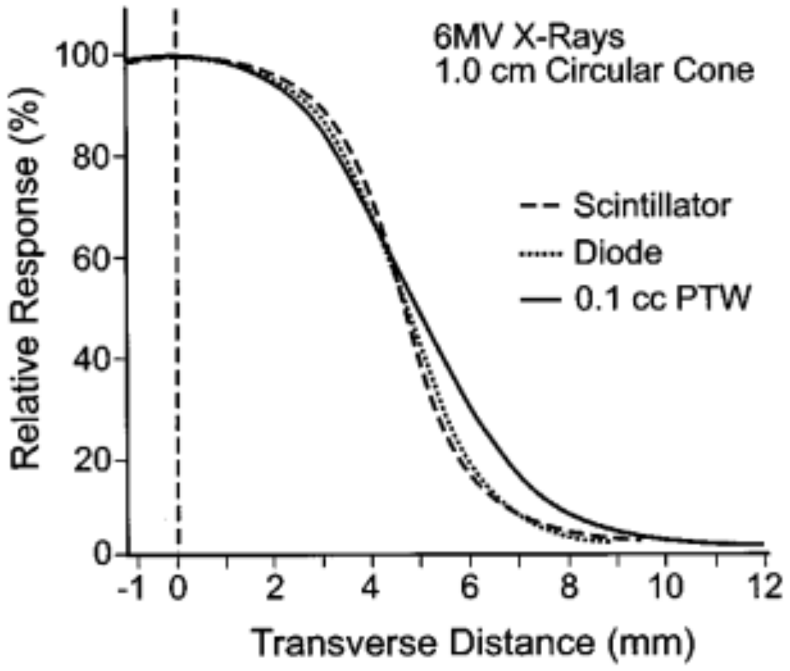

Fig. 4. Beam profile measurements made with the scintillator detector, the diode, and the 0.1-cm^3 PTW ionization chamber for the 10-mm stereotactic cone.

Beddar S, Kinsella T J, Ikhlef A, Sibata C H, **"Miniature 'Scintillator-Fiberoptic-PMT' detector system for the dosimetry of small fields in stereotactic radiosurgery"**, *IEEE Trans. Nucl. Sci.* 48: 924-928, 2001.

In Vivo Dosimetry

SYSTEM DESIGN – An example for EBRT

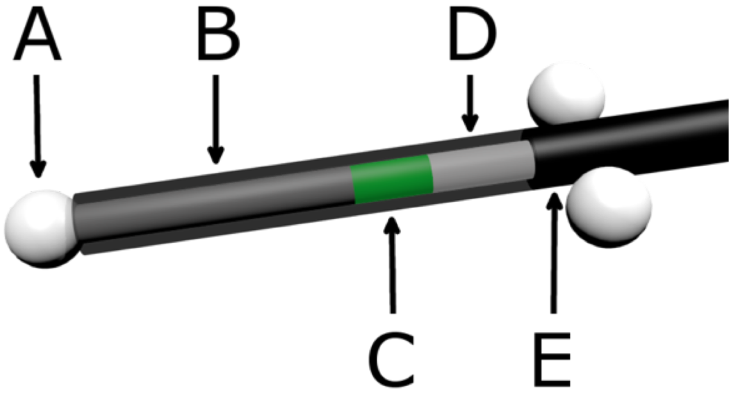

A – Ceramic fiducials

B – Carbon spacer

C – Scintillating fiber

D – Optical fiber

E – Polyethylene jacketing

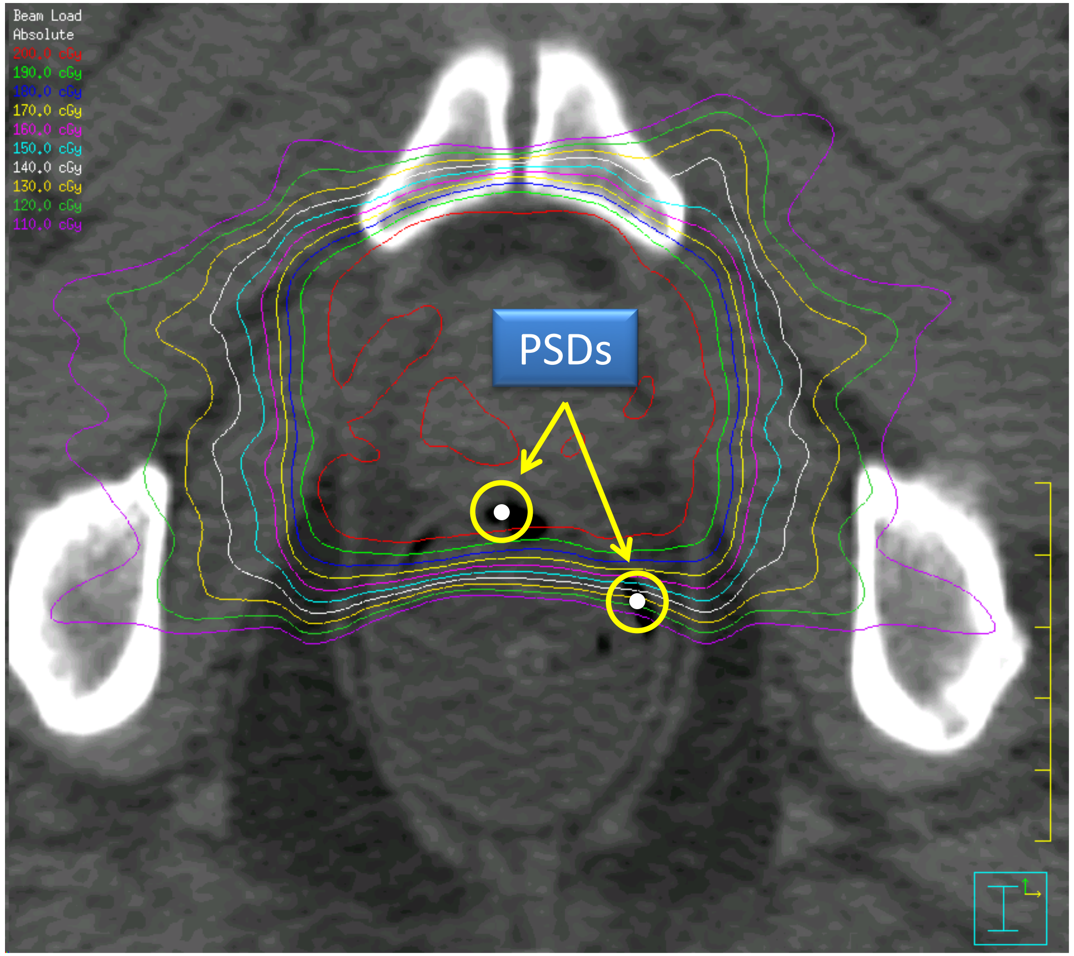

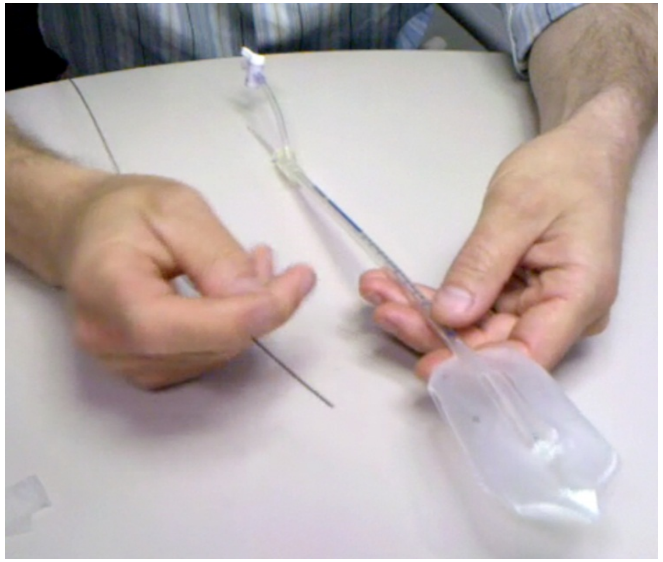

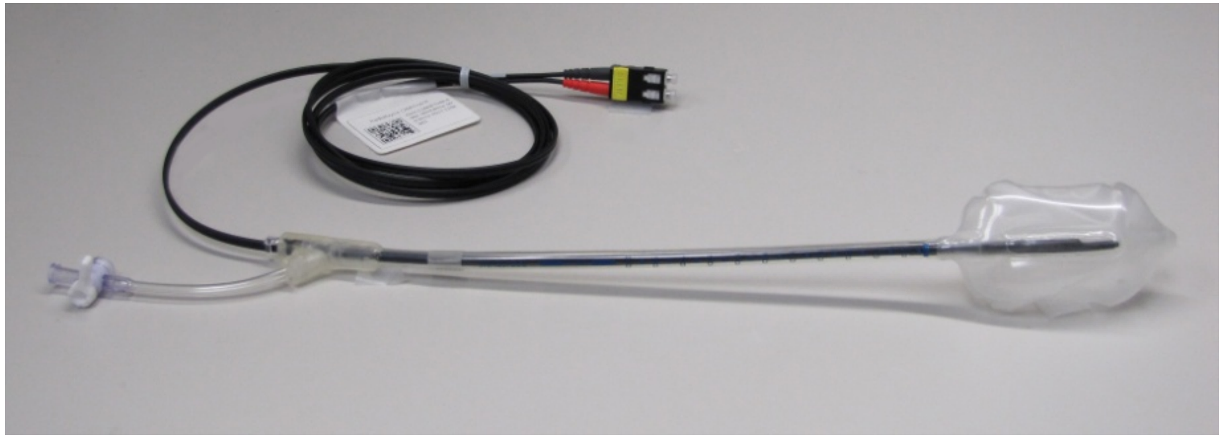

In-Vivo Dosimetry - Brachytherapy

IOP Publishing | Institute of Physics and Engineering in Medicine Physics
Phys. Med. Biol. 61 (2016) 7744–7764 doi:10.1088/

Ruby-based inorganic scintillation detectors for ^{192}Ir brachytherapy

Gustavo Kertzscher[1] and Sam Beddar[1,2,3]

[1] Department of Radiation Physics, The University of Texas MD A
Center, Houston, TX 77030, USA
[2] The University of Texas Graduate School of Biomedical Sciences
Houston, TX 77030, USA

E-mail: abeddar@mdanderson.org

Received 6 June 2016, revised 25 August 2016
Accepted for publication 19 September 2016
Published 14 October 2016

Abstract
We tested the potential of ruby inorganic scintillation detecto
in brachytherapy and investigated various unwanted lumine
that may compromise their accuracy. The ISDs were com
crystal coupled to a poly(methyl methacrylate) fiber-optic ca
coupled device camera. The ISD also included a long-pa
sandwiched between the ruby crystal and the fiber-optic cab
filter prevented the Cerenkov and fluorescence background l
induced in the fiber-optic cable from striking the ruby crystal
unwanted photoluminescence rather than the desired radiolu

IOP Publishing | Institute of Physics and Engineering in Medicine Physics in Medicine & Biology
Phys. Med. Biol. 62 (2017) 5046–5075 https://doi.org/10.1088/1361-6560/aa716e

Inorganic scintillation detectors based on Eu-activated phosphors for ^{192}Ir brachytherapy

Gustavo Kertzscher[1] and Sam Beddar[1,2,3]

[1] Department of Radiation Physics, The University of Texas MD Anderson Cancer Center, Houston, TX, United States of America
[2] The University of Texas Graduate School of Biomedical Sciences at Houston, Houston, TX, United States of America

E-mail: abeddar@mdanderson.org

Received 14 December 2016, revised 24 April 2017
Accepted for publication 5 May 2017
Published 26 May 2017

CrossMark

Abstract
The availability of real-time treatment verification during high-dose-rate (HDR) brachytherapy is currently limited. Therefore, we studied the luminescence properties of the widely commercially available scintillators using the inorganic materials Eu-activated phosphors Y_2O_3:Eu, YVO_4:Eu, Y_2O_2S:Eu, and Gd_2O_2S:Eu to determine whether they could be used to accurately and precisely verify HDR brachytherapy doses in real time. The suitability for HDR brachytherapy of inorganic scintillation detectors (ISDs) based on the 4 Eu-activated phosphors in powder form was determined based on experiments with a ^{192}Ir HDR brachytherapy source. The scintillation

Dr. Gustavo Kertzscher, Aarhus University Hospital

New “kids” on the block…

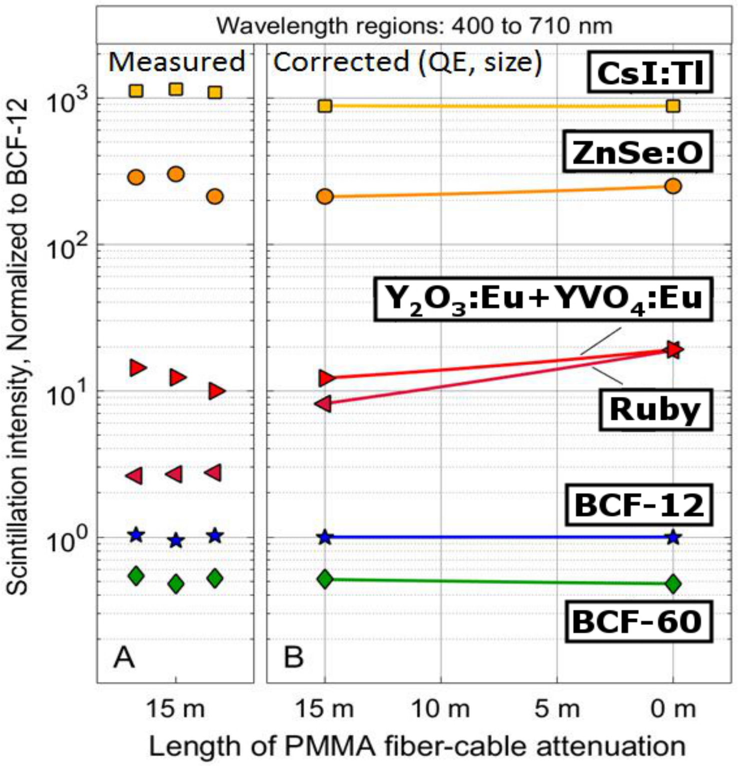

Figure 1. Measured scintillaiton intensities of the inorganic scintillation detectors with respect to BCF-12 based detectors (A) and scintillation intensities for fiber-optic cable lenghts between 0 and 15 m (B).

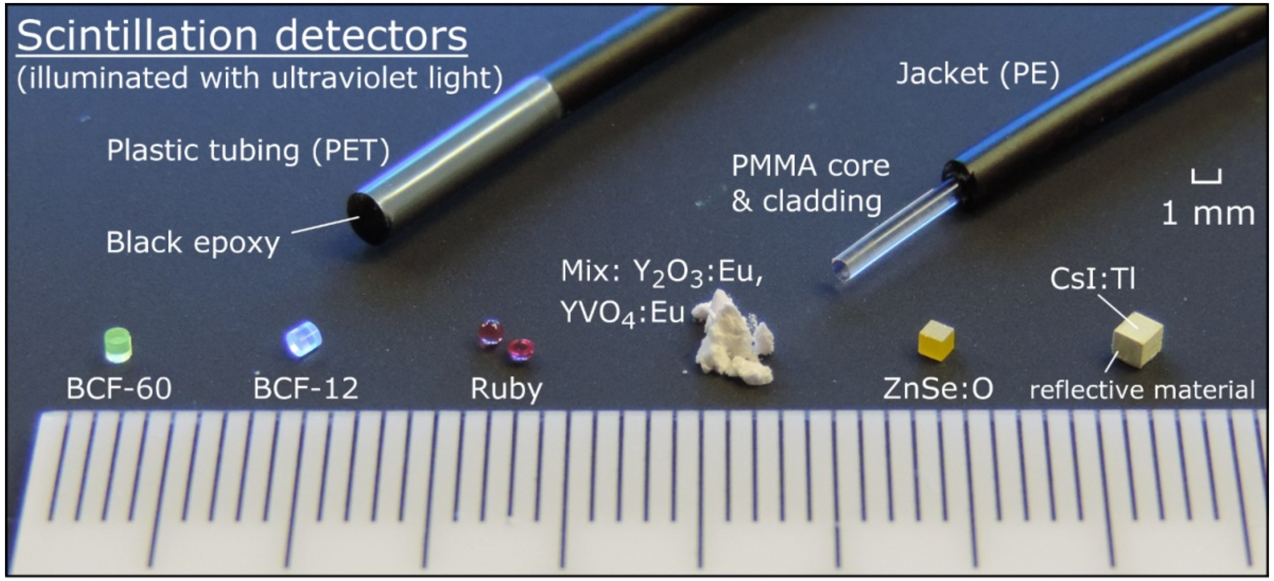

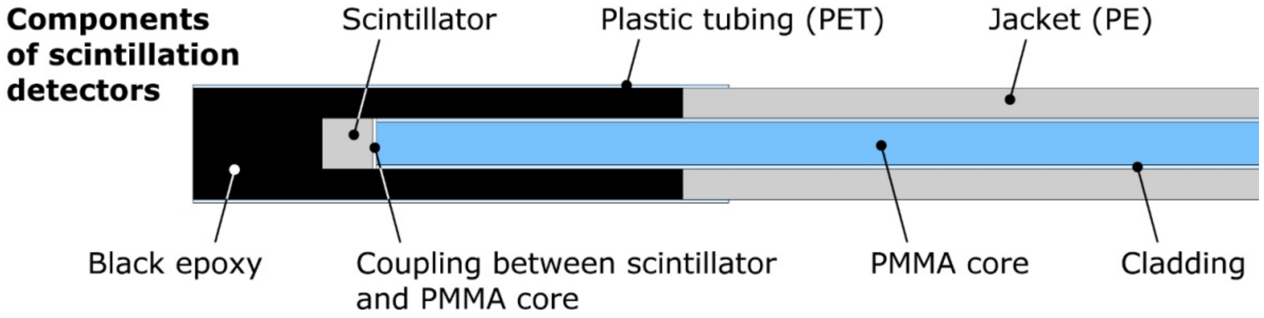

From… PSDs …to… ISDs

The MDACC in vivo dosimetry & verification system

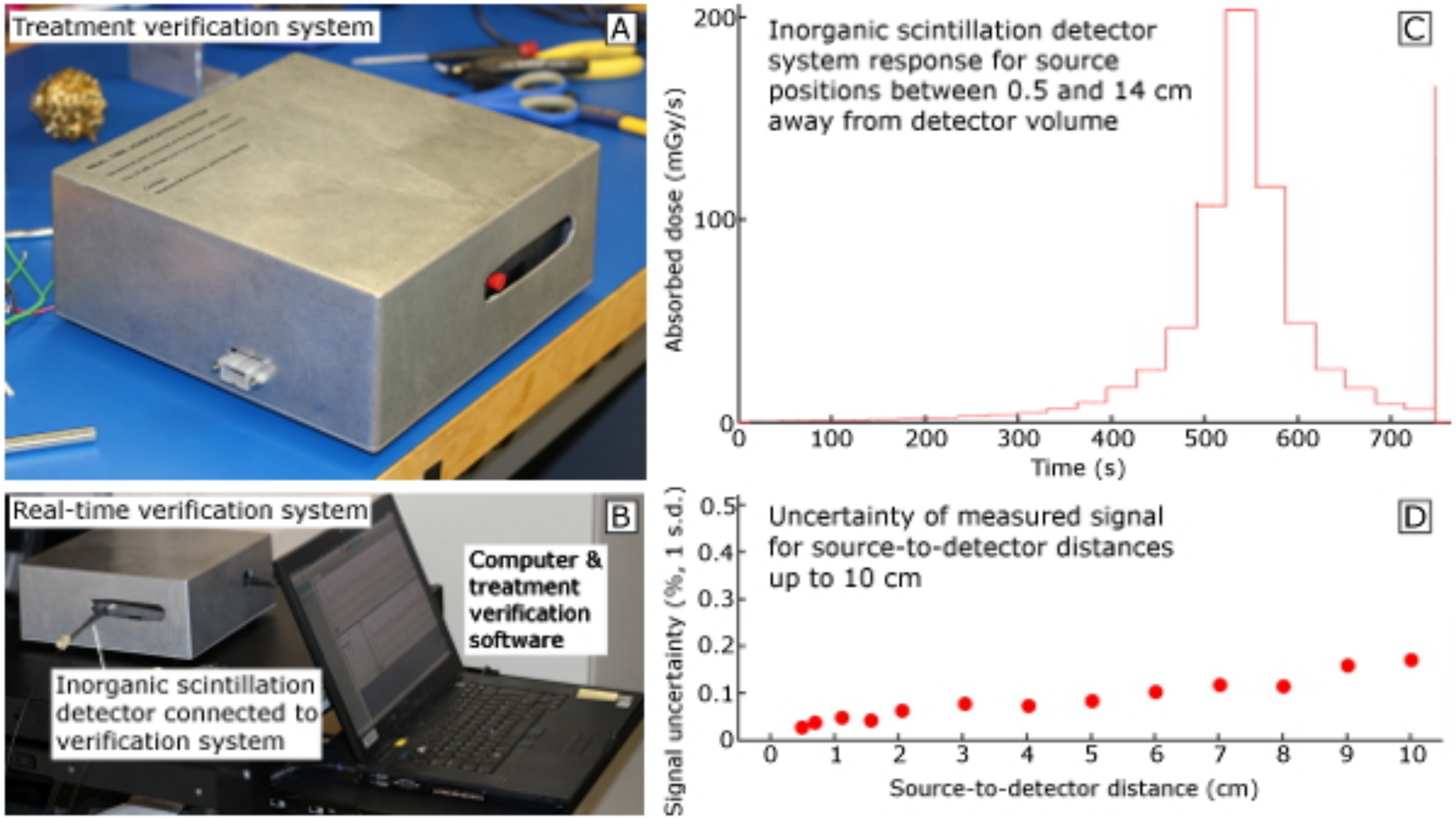

Figure 2. A. Enclosure with instrumentation for new real-time treatment verification system. **B.** Real-time treatment verification system and operating software. **C.** Time-resolved dose rates measured at 20 s^{-1} sample rate with treatment verification system and inorganic scintillation detector. **D.** Measurement uncertainty of 1-second signal accumulation.

Volumetric (3D) Dosimetry

Concept of the 3D Detector

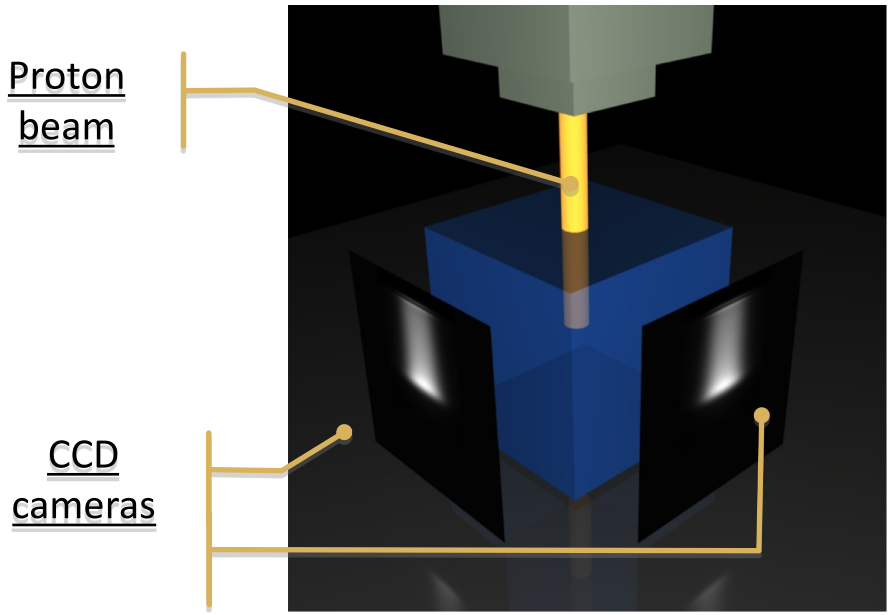

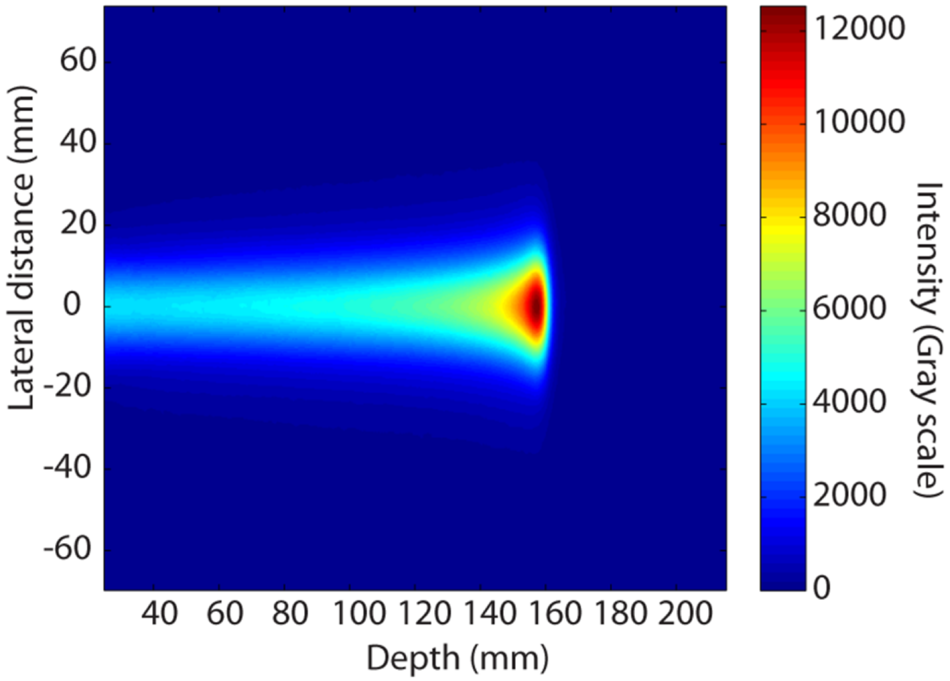

- Liquid scintillator: OptiPhase Hi-Safe 3
  - Diisopropyl naphthalene solvent and PPO fluor w/ bisMSB wavelength shifter
  - Density: 0.963 g/cm^3
  - Peak emission: ~430 nm
  - Light emission decay time: < 20 ns

Measurement Procedure

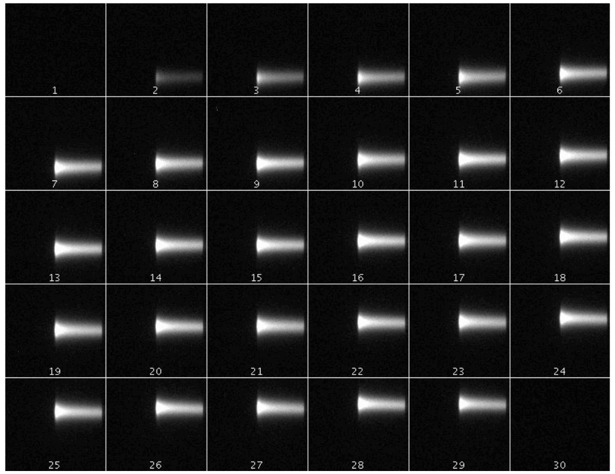

Image acquisition coordinated with beam delivery

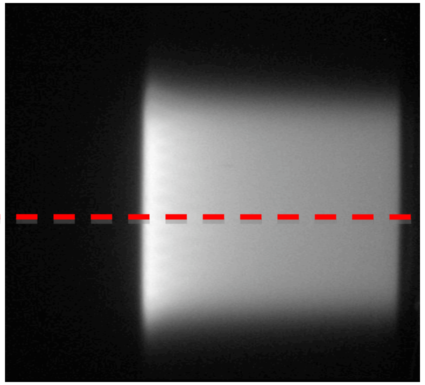

Sum of spots for one energy layer

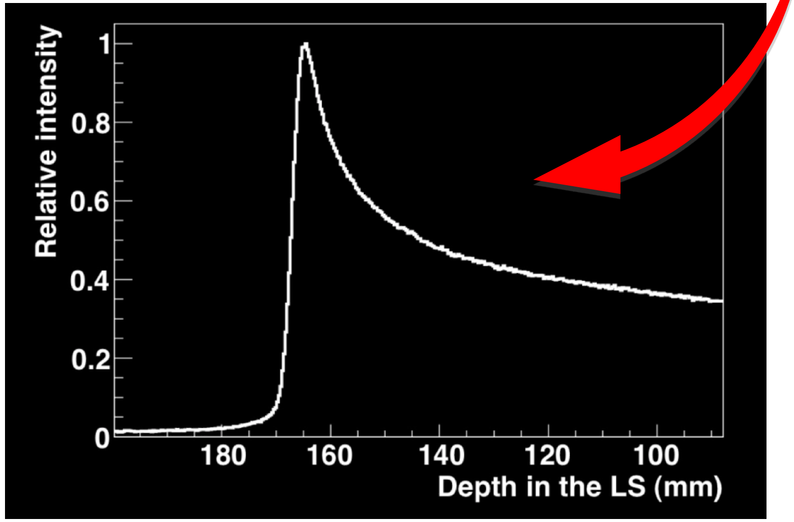

In each image frame

- Measure proton range
- Measure spot position
- Measure spot intensity

Volumetric Scintillation Dosimetry

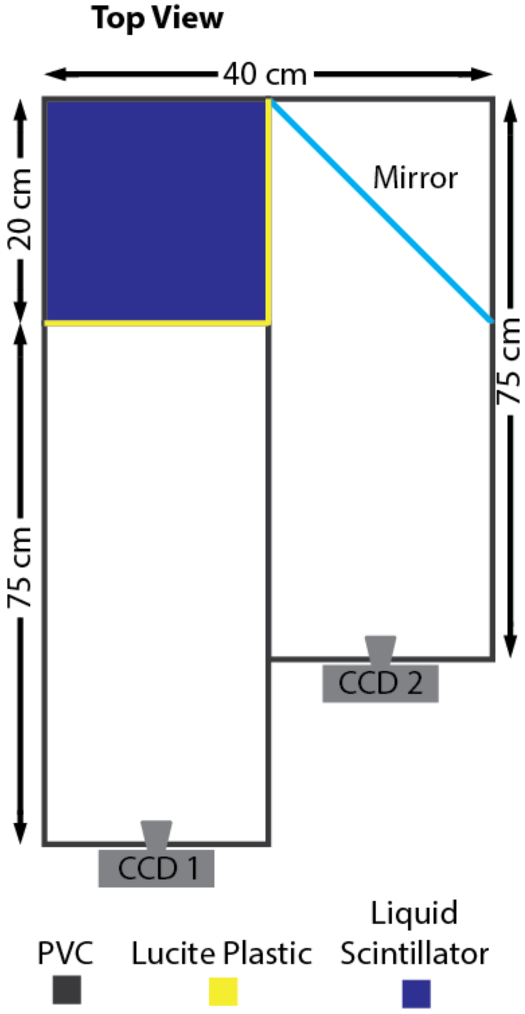

Beam's eye view (CCD 2)

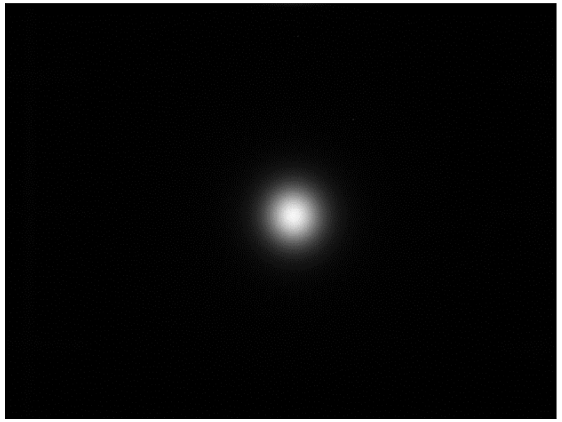

Lateral view (CCD 1)

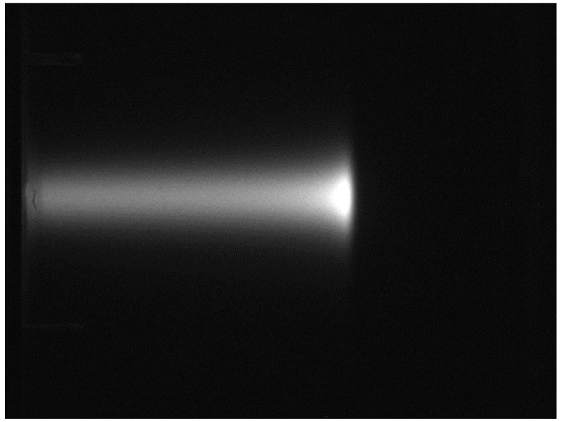

Volumetric Scintillation Dosimetry

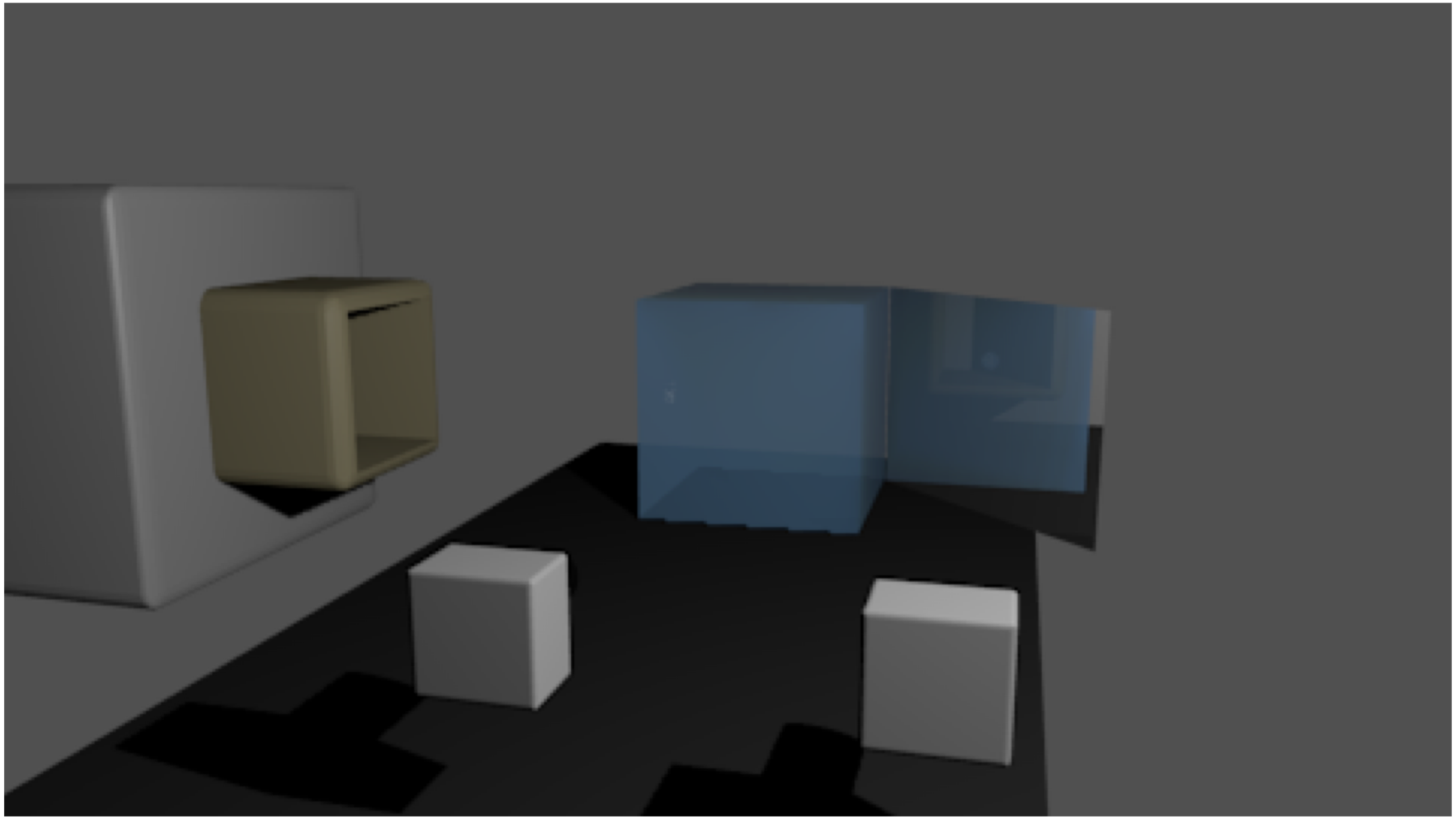

Courtesy of Daniel Robertson

Scintillation Dosimetry

IOP Publishing | Institute of Physics and Engineering in Medicine   Physics in Medicine & Biology
Phys. Med. Biol. 62 (2017) 5652–5667   https://doi.org/10.1088/1[illegible]1-6560/aa78[illegible]

Performance characterization of a 3D liquid scintillation detector for discrete spot scanning proton beam systems

Chinmay D Darne[1], Fahed Alsanea[1], Daniel G Robertson[2], Narayan Sahoo[1] and Sam Beddar[1,3]

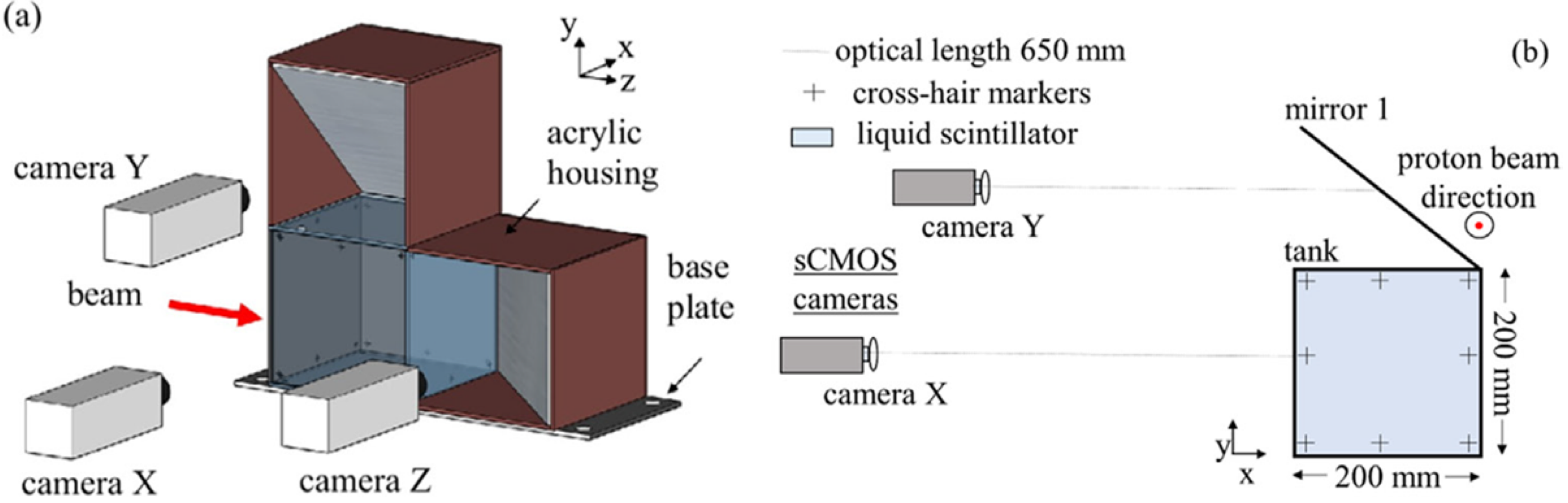

Actual System Setup

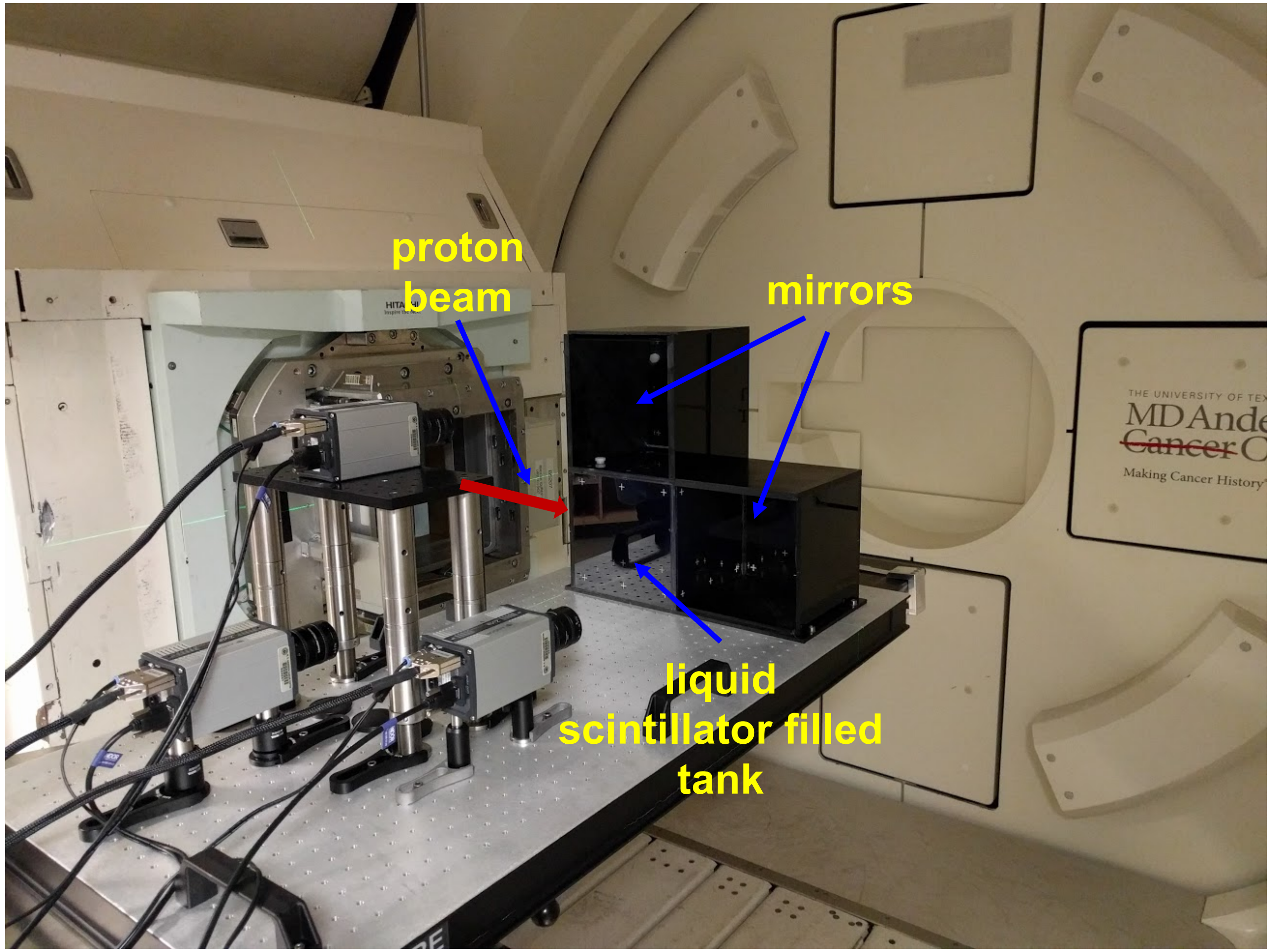

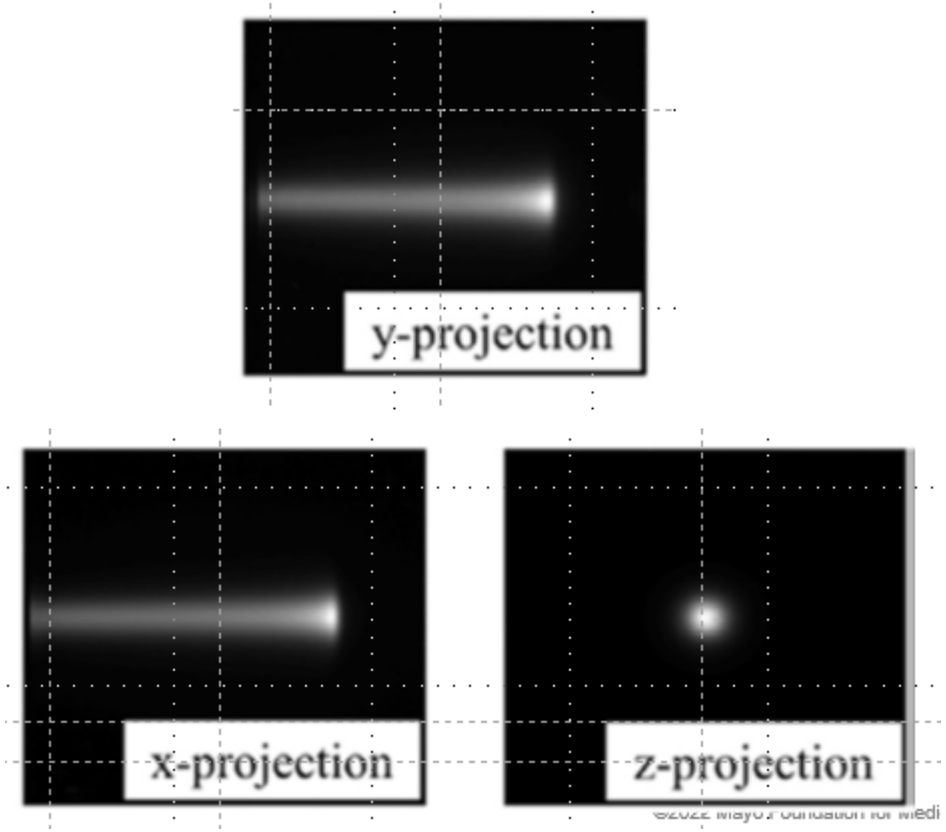

Darne C D, Alsanea F, Robertson D G, Sahoo N and Beddar S Performance characterization of a 3D liquid scintillation detector for discrete spot scanning proton beam systems, Phys. Med. Biol. 62 (2017), 5652-67

Imaging Patient Treatment Plans

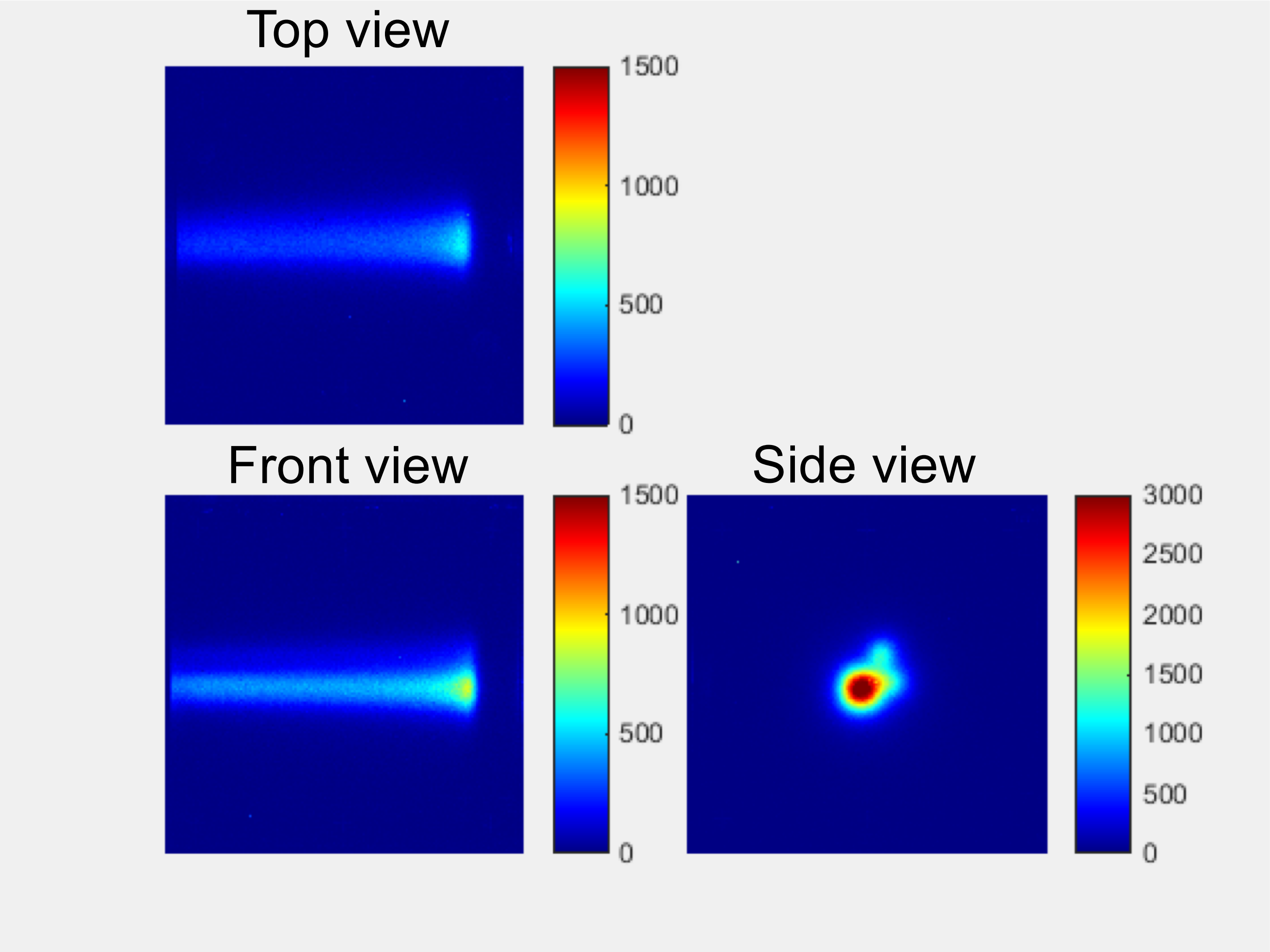

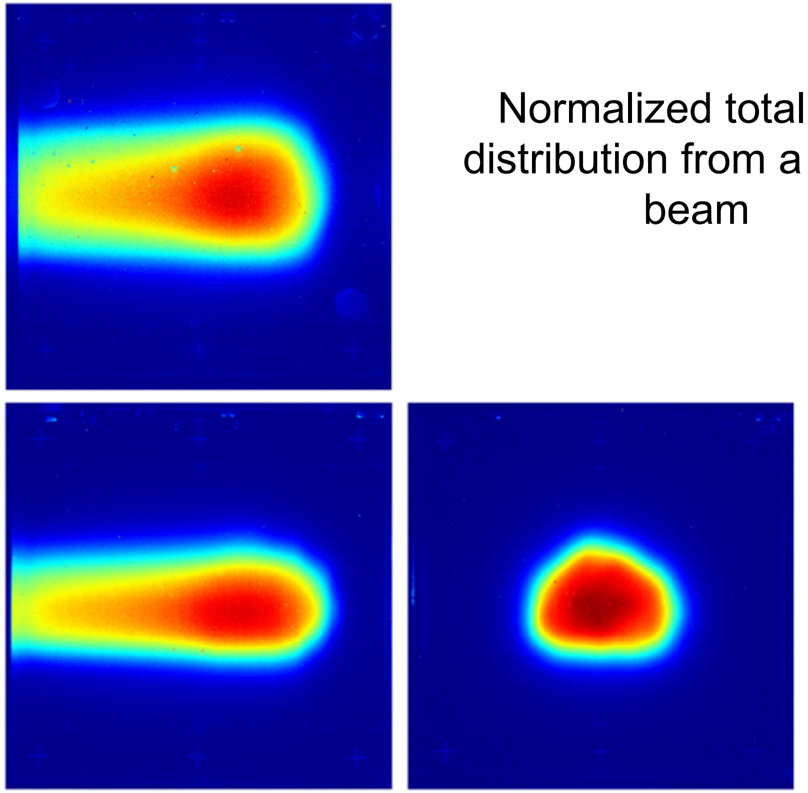

Normalized total light distribution from a lateral beam

- Prostate treatment plan (1 lateral beam)
- 17 total energies: 163.9 MeV – 203.7 MeV
- 40 MU total delivered dose

Proton-integrating CT & Radiography

Proton Radiography Detectors Types

Range Telescope/List mode

Pro

- Spatial resolution
- Lowest dose
- Existing equipment
- Simple device
- Clinical beam
- Fast imaging

Con

- Complex/Expensive
- Non-clinical beam mode
- Resolution less than single particle
- Higher dose
- Slower than single particle
- Dose higher than single particle

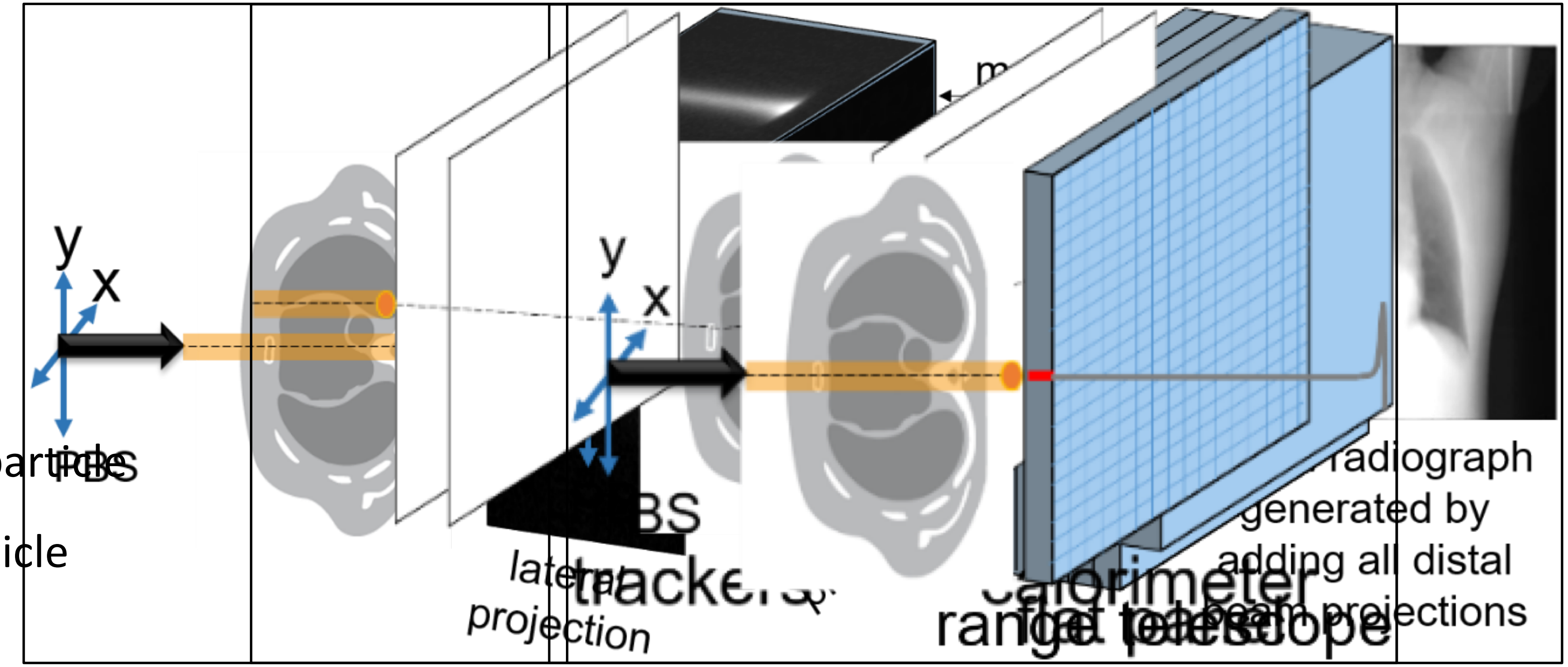

Courtesy Daniel Robertson

Imaging with a Large Scintillator

- Shoot proton beam through object into a large scintillator
- Beam's-eye-view camera measures light distribution
  - ➢ Intensity correlated to proton range
- Lateral cameras provide additional information

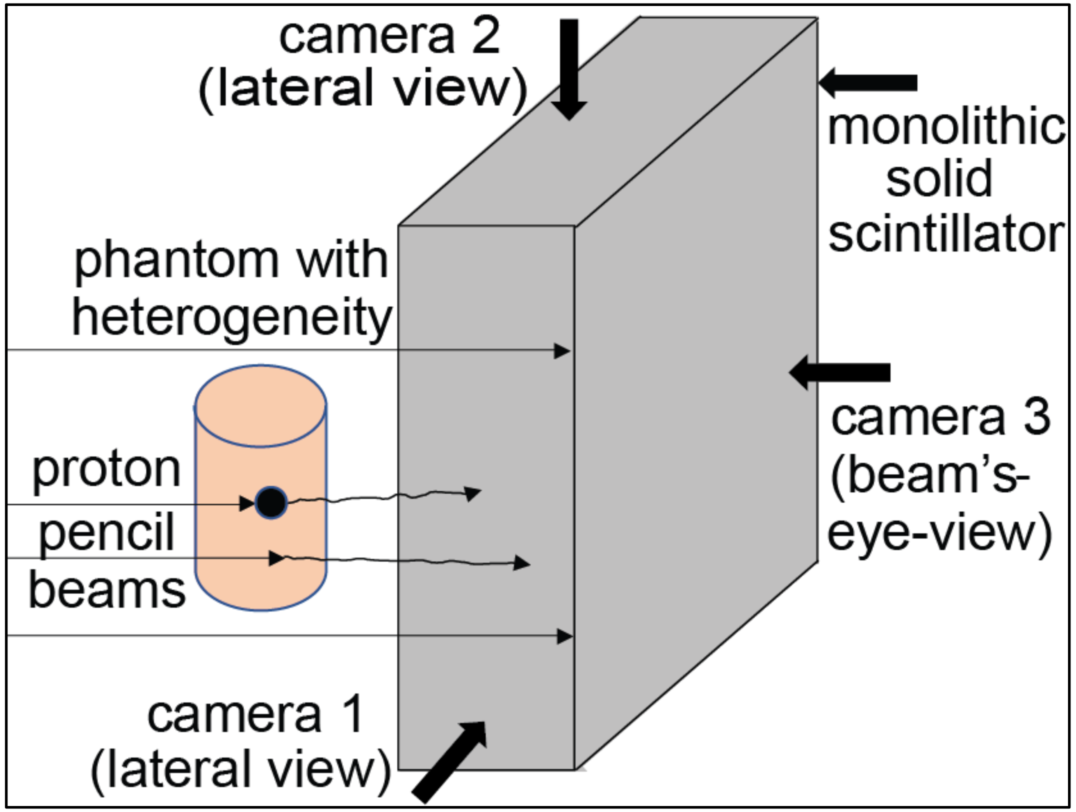

What is the Motivation

And why Scintillators and Cameras

- **It's what we know**
- **Simplicity and cost**

  "Off-the-shelf" electronics

  Few components

  Simple assembly and operation
- **Clinical integration**

  Clinical beam delivery mode (no beam tuning for low fluence)

  Fewer detector elements (distal only)

Integrative Proton Radiography

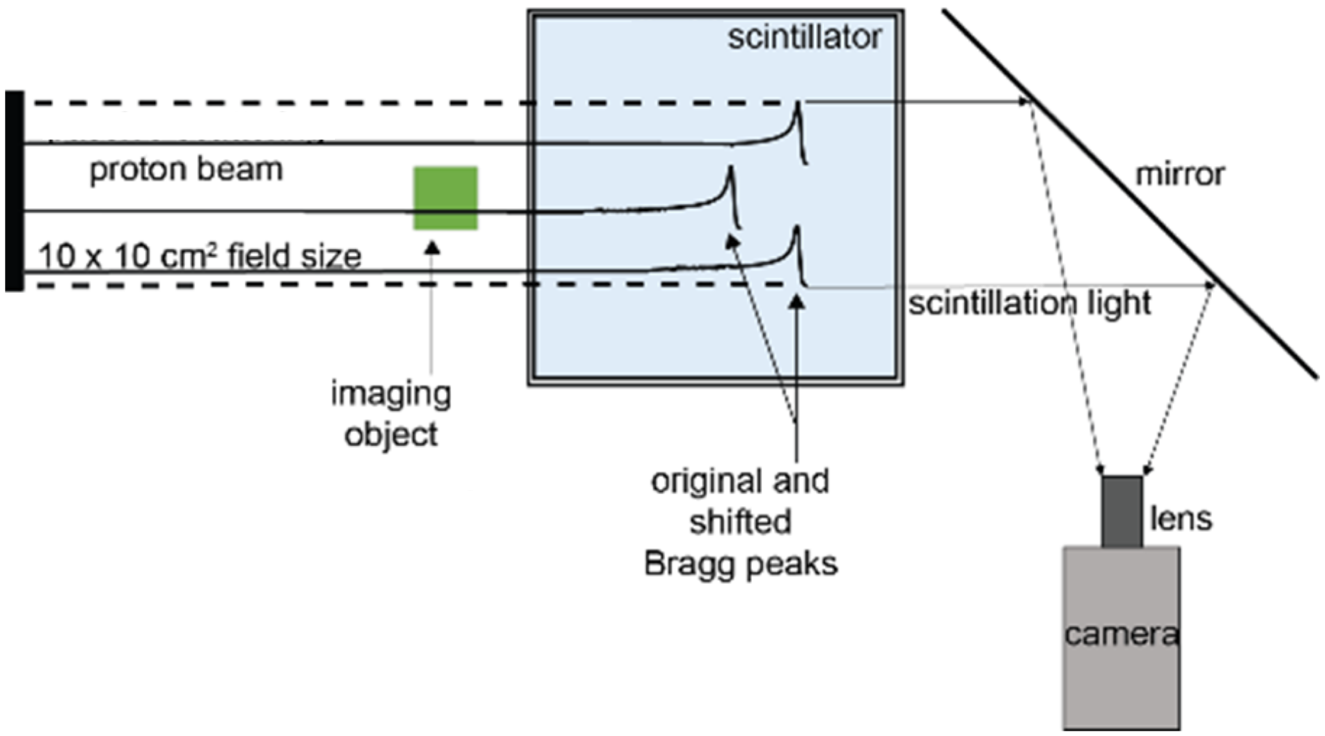

- Schematics of a proton radiography system used for preliminary studies.

- A normalized proton beam Bragg curve is pulled back by a depth equivalent to the cube's water equivalent thickness.
- The cumulative intensity curve measured by camera 3.

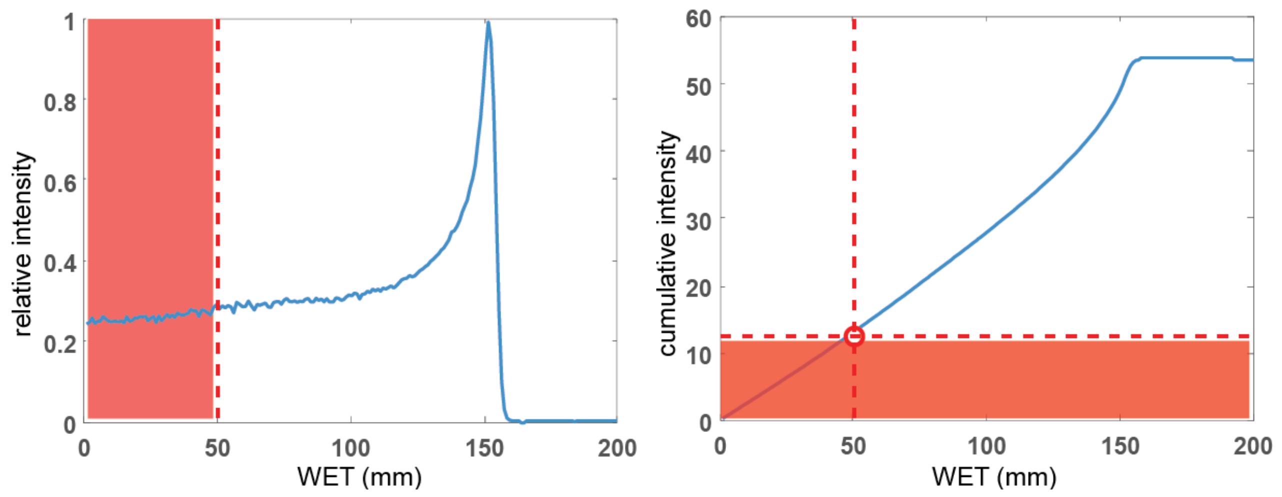

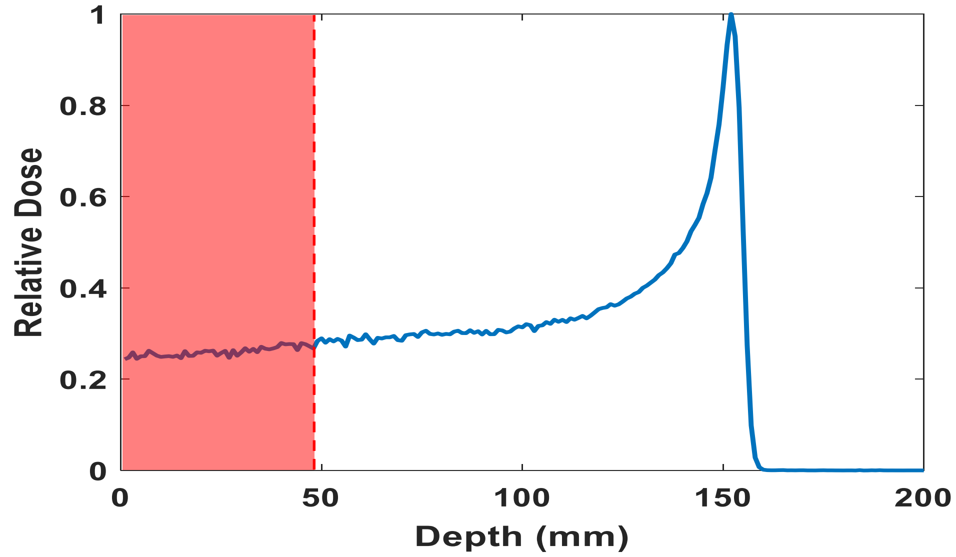

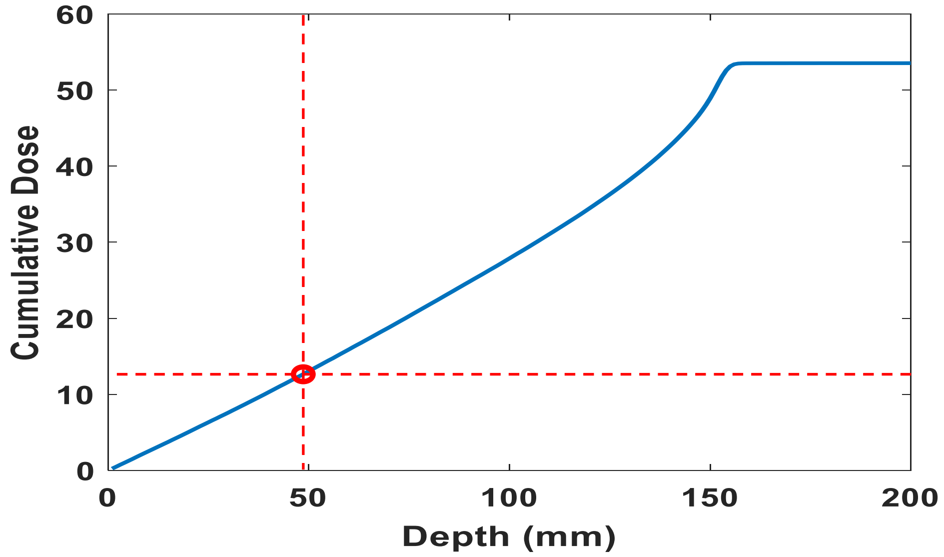

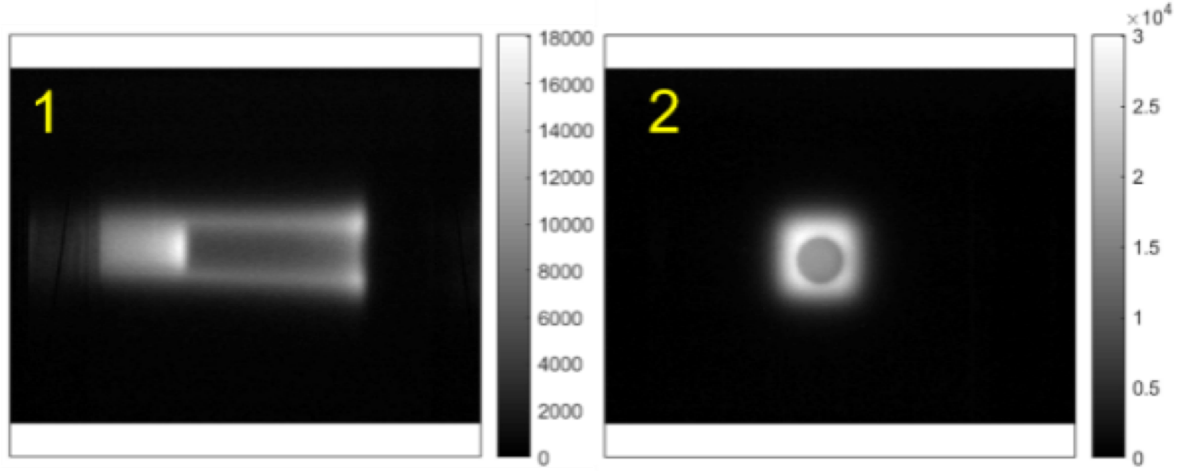

- Cumulative light signal in the depth direction is measured by the XY projection.
- Proton beam transit through an object pulls back the Bragg peak, yielding a decrease in the cumulative light signal in the XY projection.
- The depth on the cumulative light signal corresponding to the lost intensity is equal to the water equivalent thickness of the object.

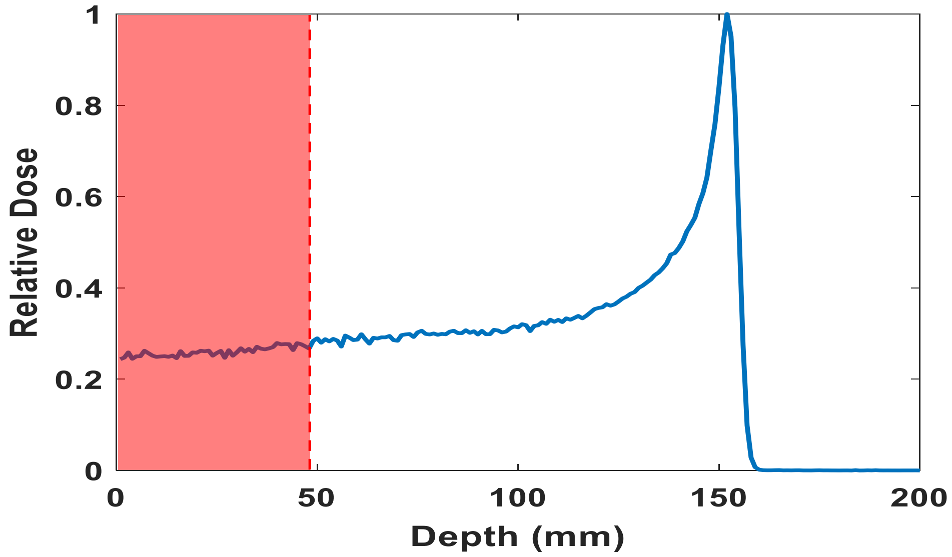

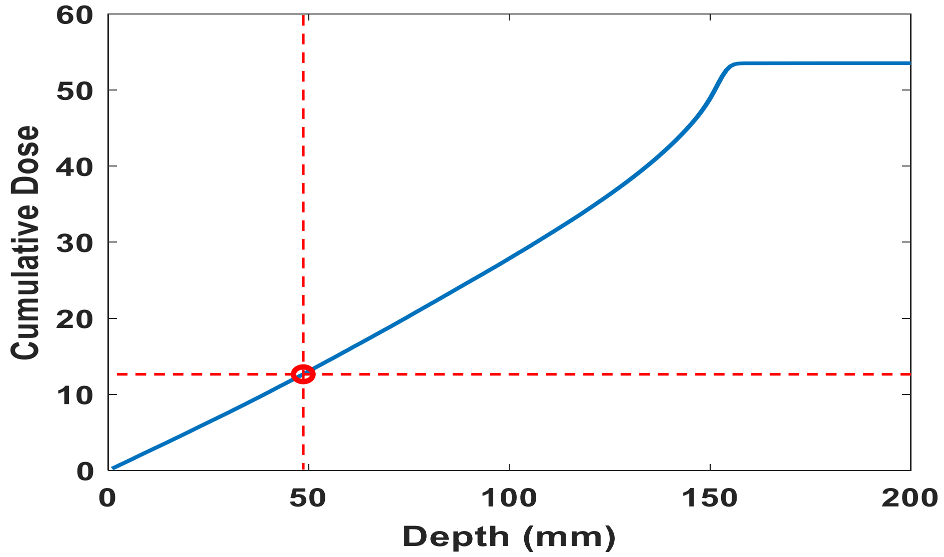

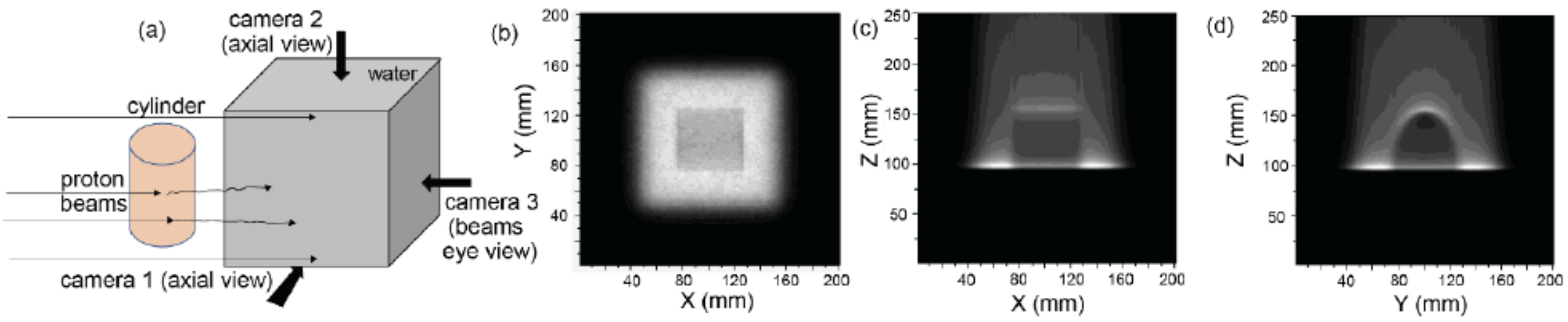

- The set-up used for the simulation.
- A proton radiograph obtained by camera 3.
- (c and d) The light distribution projections captured by camera 1 and 2, respectively.

Experimental Testing of the pRad Concept

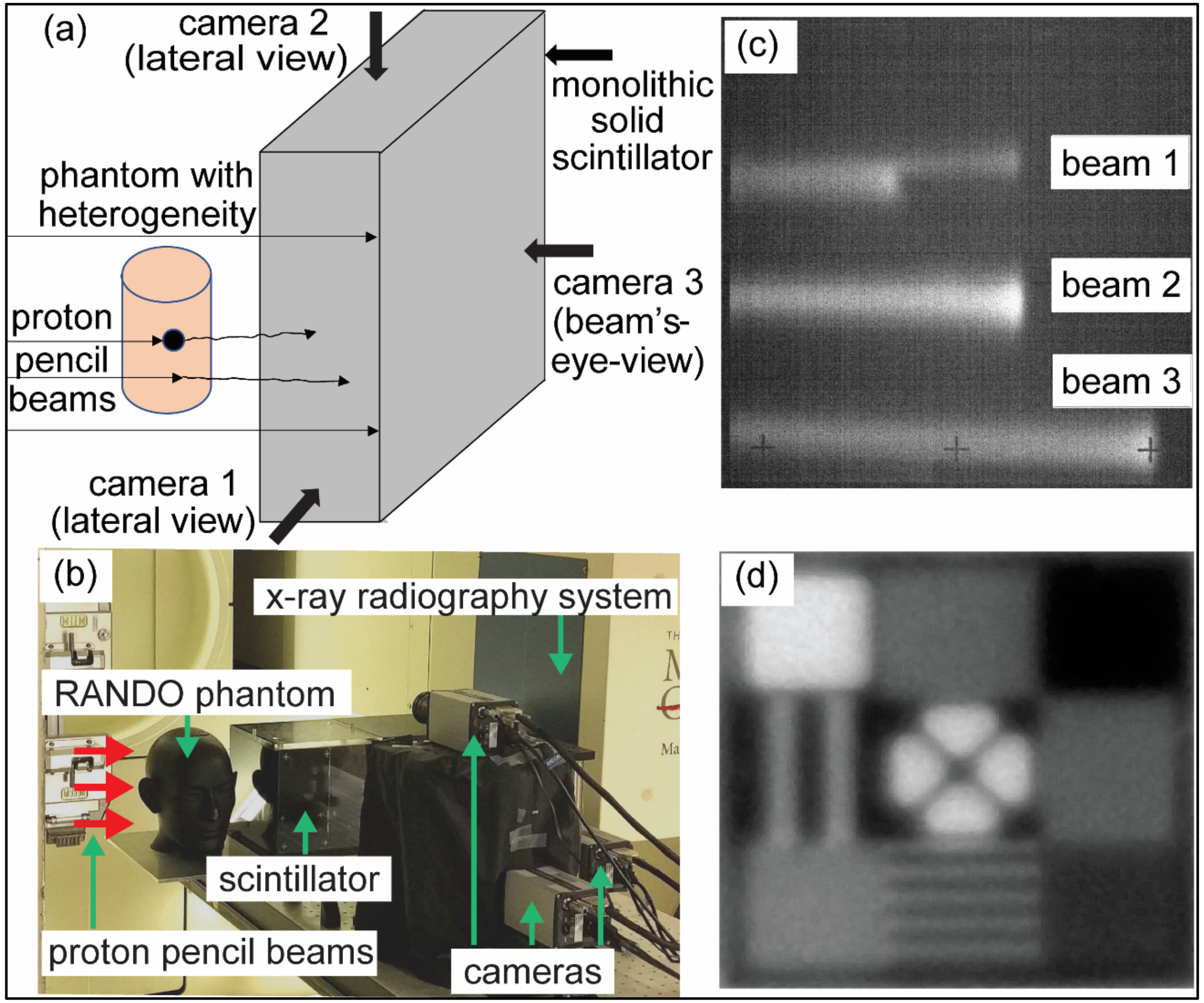

(a) A schematic of the proposed proton radiography system. The scintillation light produced within the solid scintillator in response to the proton beams was captured by 3 digital cameras from 3 mutually perpendicular directions. Camera 3, placed along the beam's-eye-view direction, generated the proton radiograph by integrating the light fluence. Cameras 1 and 2 generated lateral beam images that captured the beam location, divergence, and its residual range within the scintillator.

(b) (b) A photograph of the modified 3D dosimetry system for experimental testing of the radiography concept. **This experimental setup used a volumetric liquid scintillator (OptiPhase HiSafe3, PerkinElmer, Waltham, MA) enclosed in a 20-cm^3 tank.** A 168.8-MeV beam energy was selected for imaging.

(c) (c) A raw projection image of the lateral view of 3 pencil beams (captured using camera 1).

(a) (d) A proton radiograph of an MV-QA phantom imaged using a passively scattered 160 MeV proton beam.

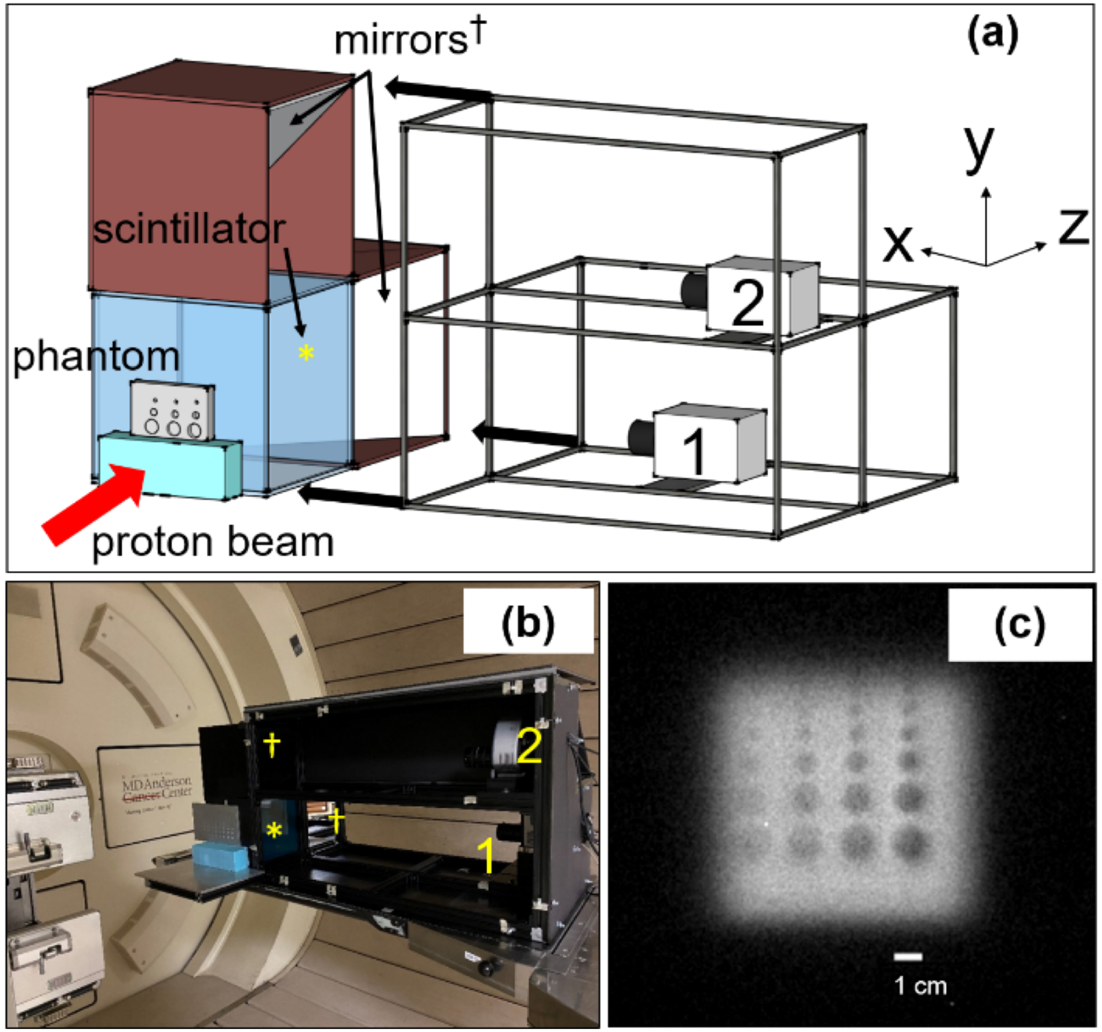

(a) Schematic of the prototype pRAD system. **This setup uses a 20-cm^3 EJ-260 (Eljen Technology, Sweetwater, TX) monolithic solid scintillator volume** and 2 cameras.

(b) A photograph of the system placed on the patient couch within the proton gantry. Black foam panels mounted around the system minimize ambient light contamination.

(c) A proton radiograph of the Las Vegas phantom generated using a 163-MeV proton beam.

Physics in Medicine & Biology

IPEM Institute of Physics and Engineering in Medicine

PAPER

CrossMark

RECEIVED
31 October 2020

REVISED
16 June 2021

ACCEPTED FOR PUBLICATION
18 June 2021

PUBLISHED
9 July 2021

Image quality evaluation of projection- and depth dose-based approaches to integrating proton radiography using a monolithic scintillator detector

Irwin Tendler[1], Daniel Robertson[2], Chinmay Darne[1], Rajesh Panthi[1], Fahed Alsanea[1], Charles-Antoine Collins-Fekete[3] and Sam Beddar[1,4,*]

Purpose

Compare the image quality of an integrating proton radiography (PR) system, composed of a monolithic scintillator and two digital cameras, using integral lateral-dose and integral depth-dose image reconstruction techniques.

- MC simulation of energy deposition to create pRs of various phantoms: a slanted aluminum cube for spatial resolution analysis and a Las Vegas phantom for contrast analysis.
- The light emission of the scintillator was corrected for quenching using Birks scintillation model.
- list-mode single-particle tracking pR was used for reference data (Deffet 2018, Darne et al 2019, Deffet et al 2020).

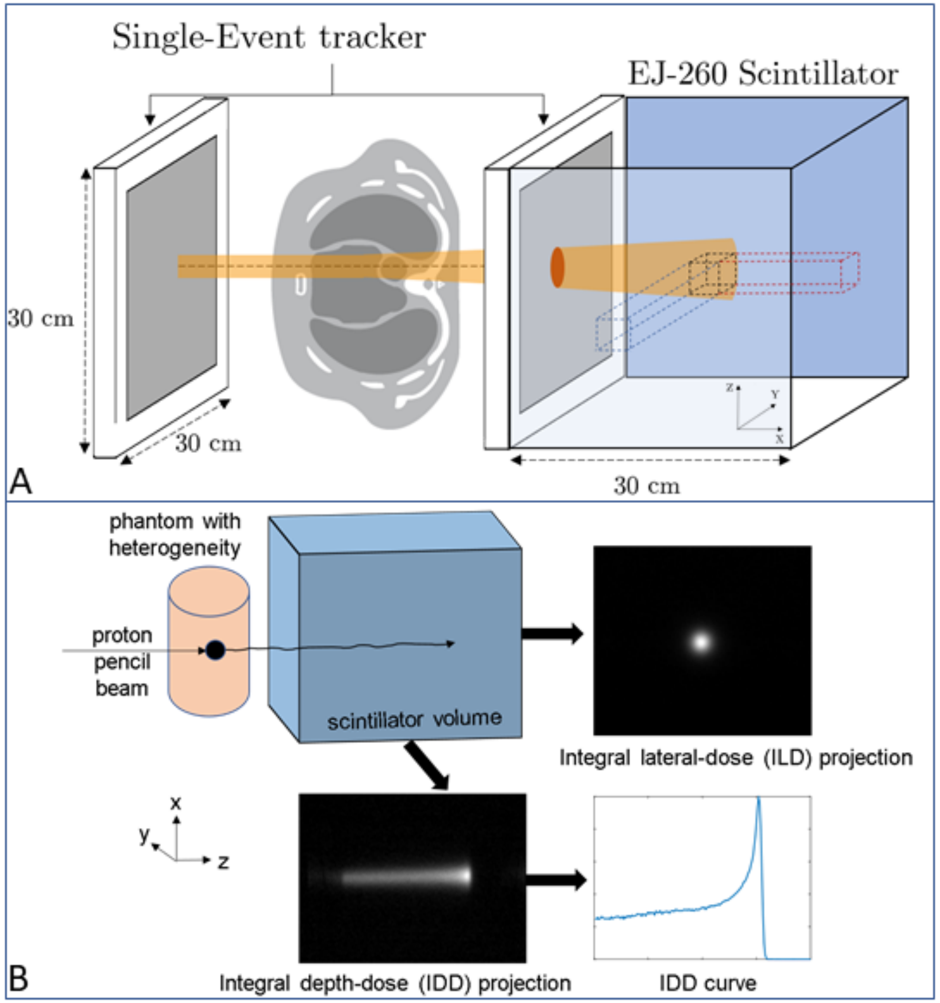

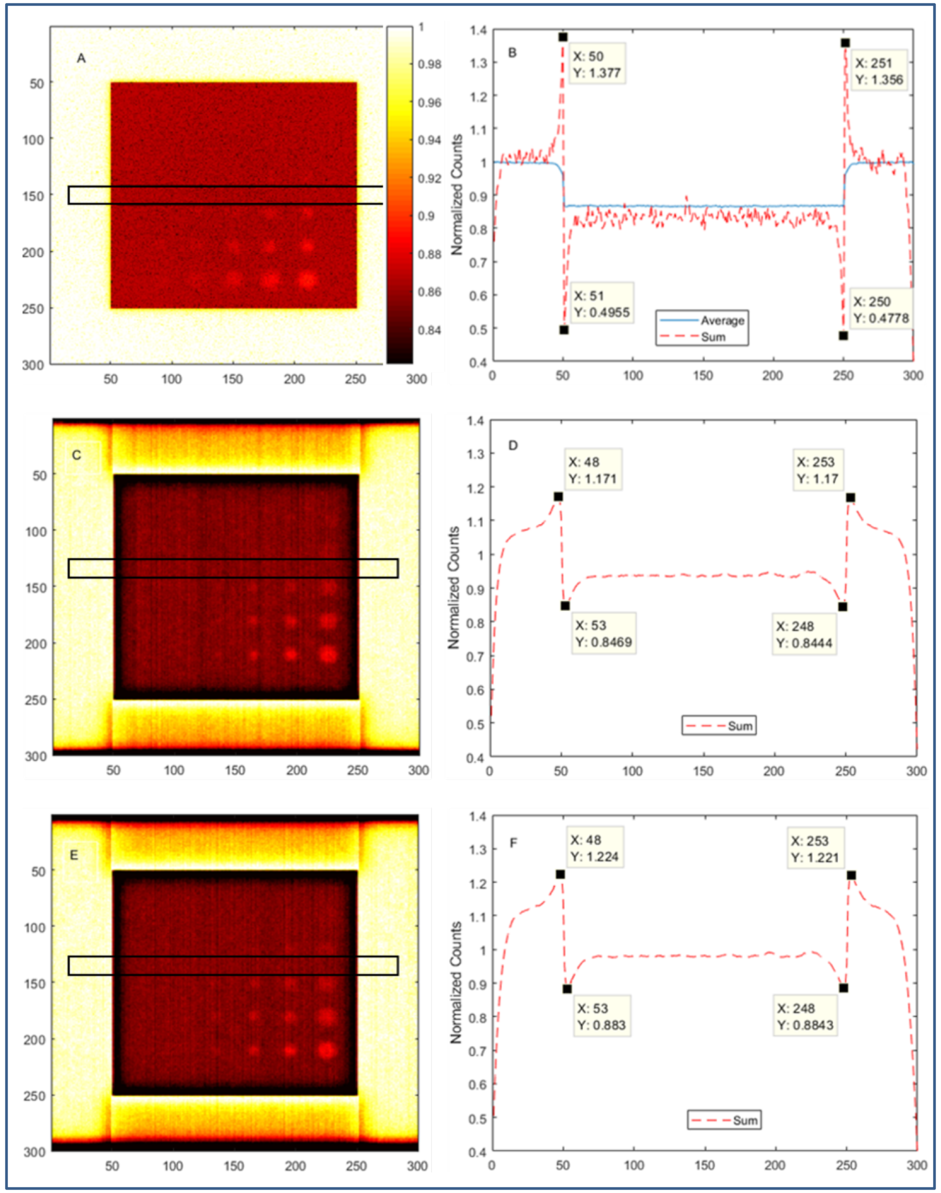

(A) Cumulative image of Las Vegas phantom generated using 100 x 100 pencil beams (7.05 mm FWHM) normalized to the maximum intensity pixel value. (C) Cumulative image produced using half beam spacing (200 x 200 pencil beams), corresponding summed line profile is shown in (D)

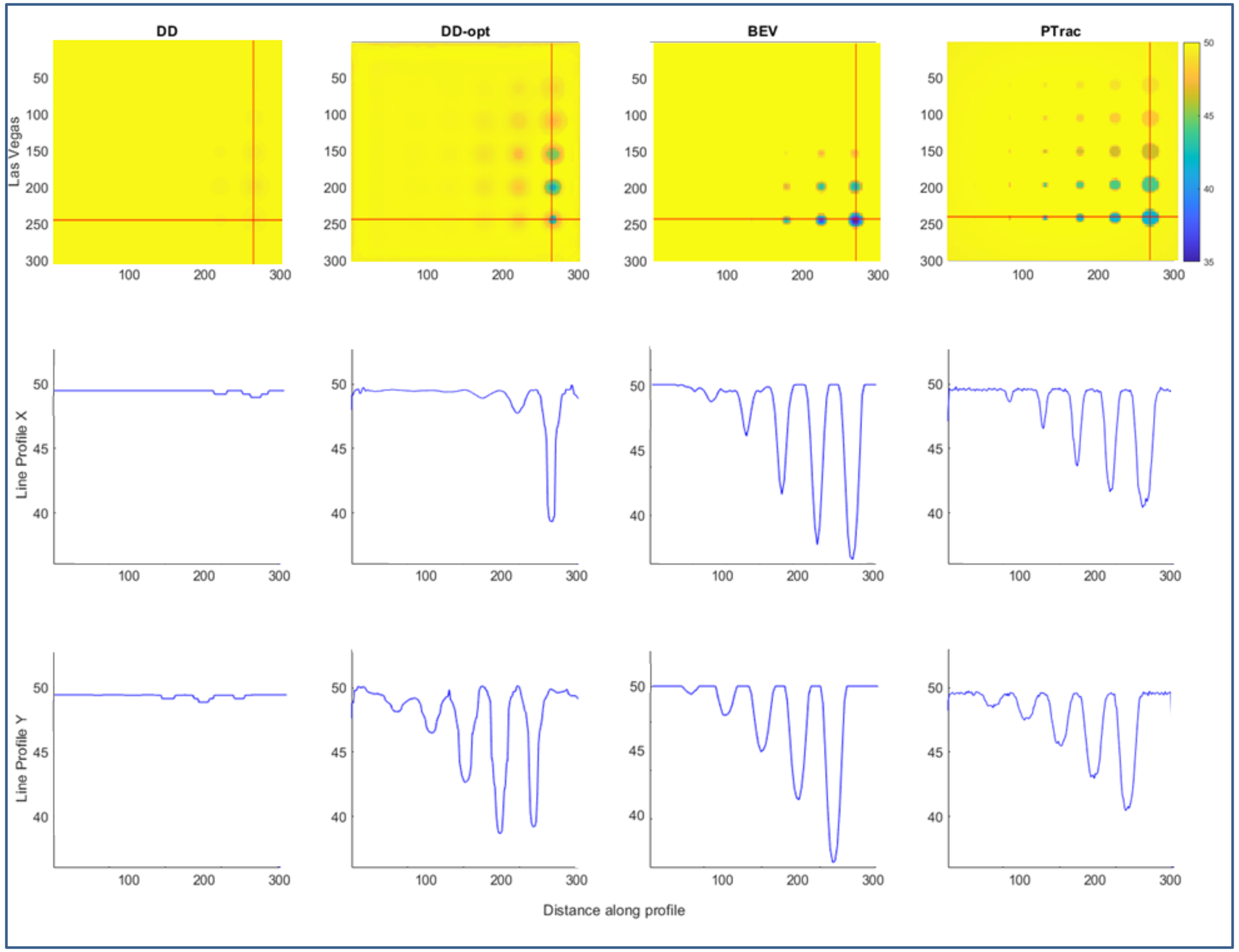

Row 1 shows reconstruction results of depth-dose (DD), depth-dose-optimized (DD-opt), beam's eye view (BEV), and single particle tracking (PTrac) for a Las Vegas phantom. Row 2 and 3 show x and y line profiles respectively. Distance along profile is in units of pixels. Colorbar is shown in units of WET (mm) and is applicable to all Las Vegas phantom images.

Experimental Studies

Detector design

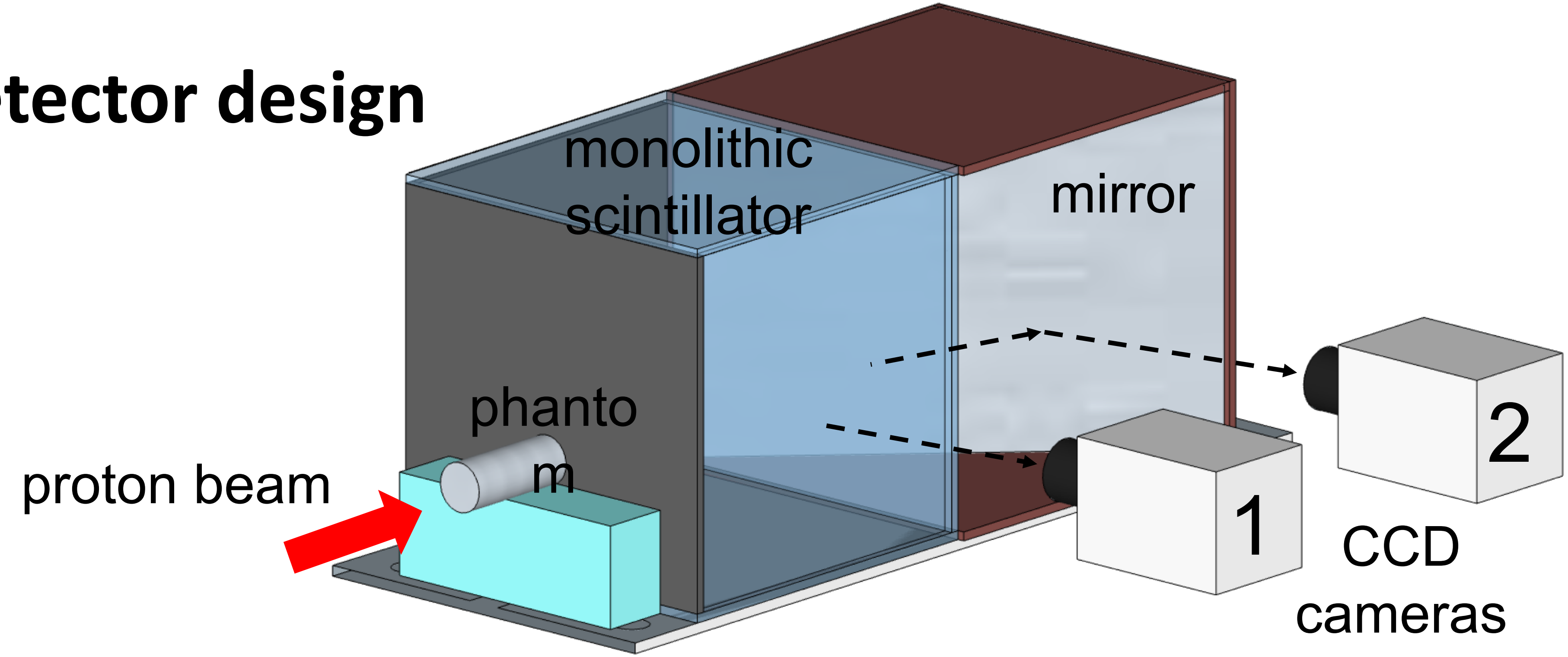

The monolithic scintillator detector (20 × 20 × 20 cm^3) generates light which is captured by 2 CCD cameras: We used 164 MeV (18 cm range) pencil beams to generate radiographs. Dashed lines indicate optical paths from scintillator to cameras.

Four Gammex cylindrical phantoms (7 cm long and diameter 2.8 cm) were selected for imaging

CD Darne, DG Robertson, F Alsanea, C-A Collins-Fekete and S Beddar, A novel proton-integrating radiography system design using a monolithic scintillator detector: Experimental studies, NIMA, Vol. 1027, 2022

The Prototype Detector

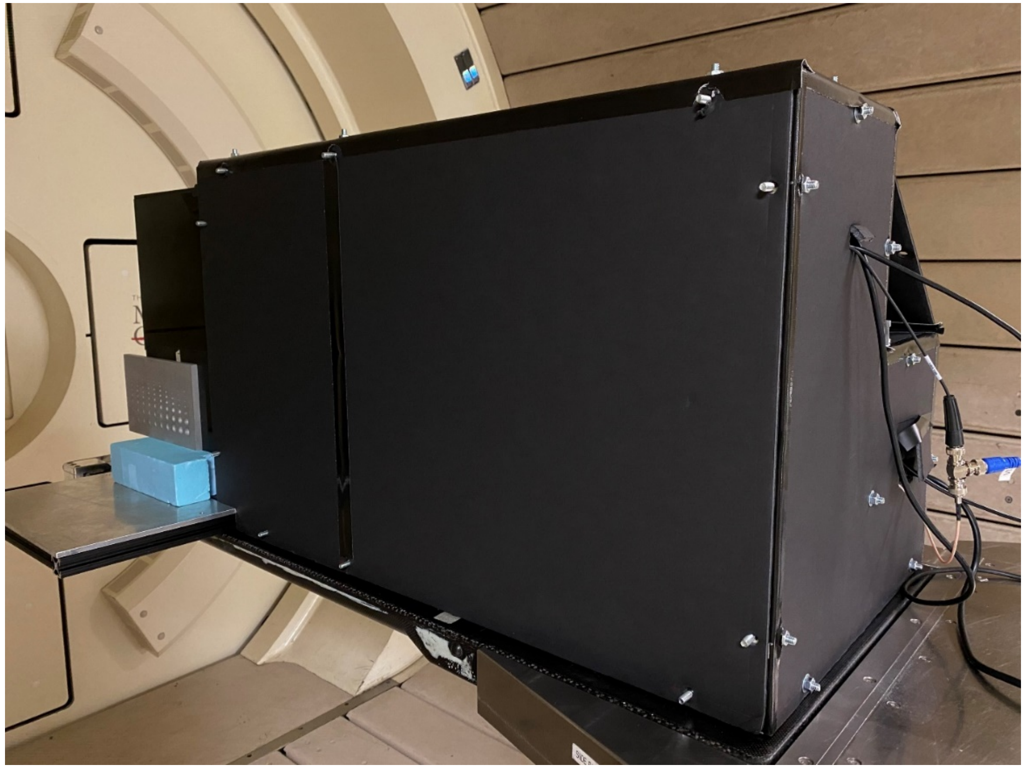

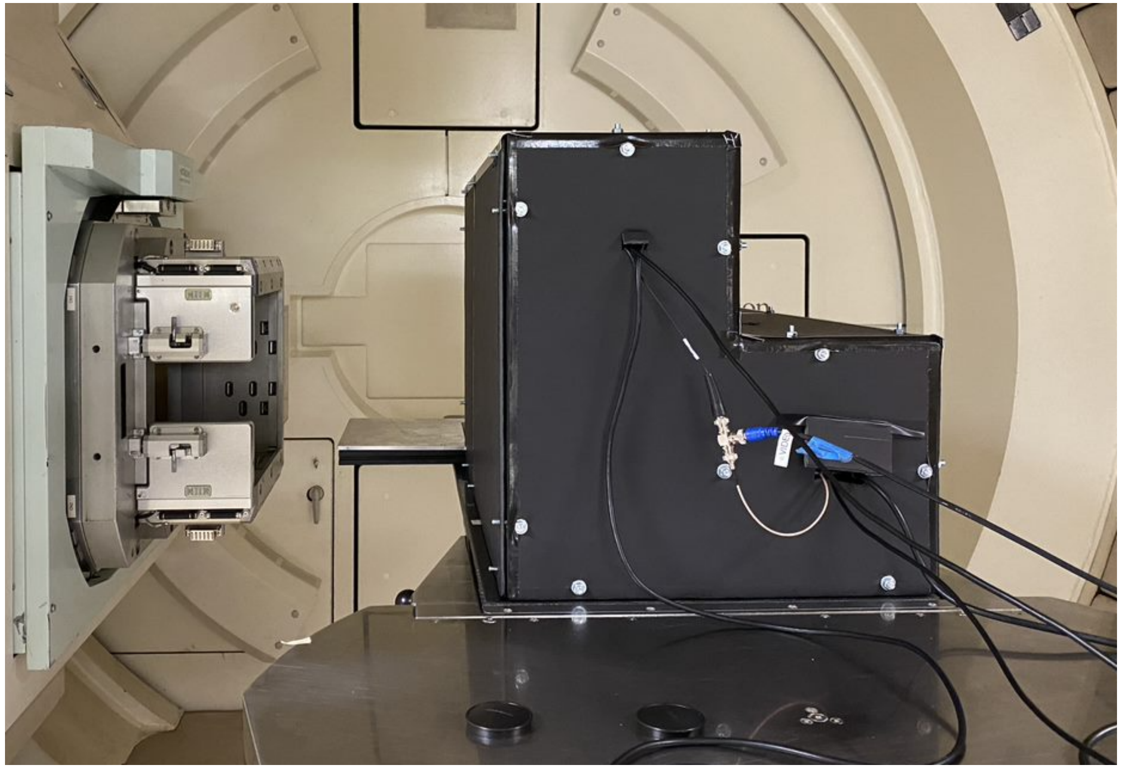

Image Quality & WET Accyracy

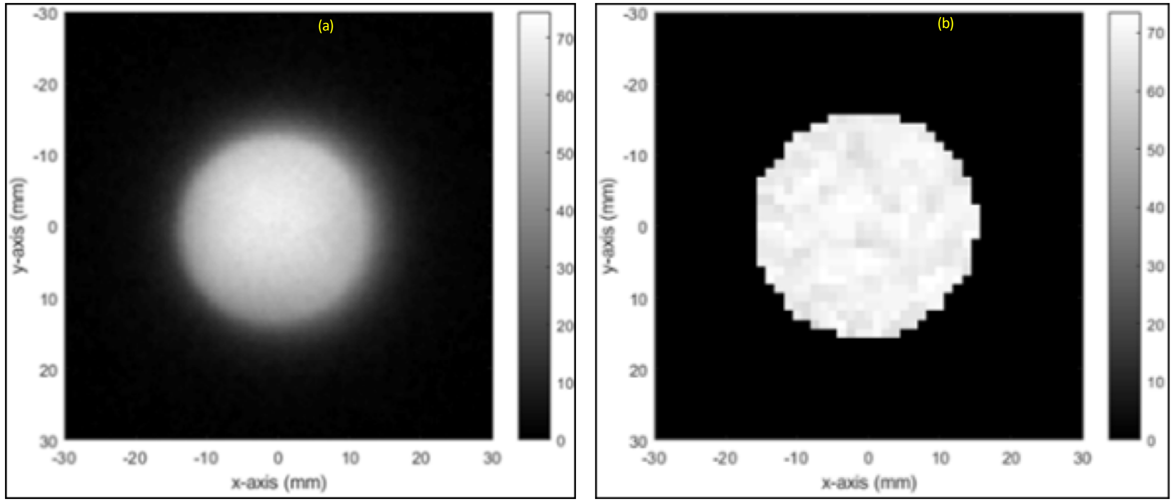

Proton radiographs of cortical bone phantom reconstructed for the solid water phantom using a pencil beam grid spacing of 2.5 mm with

(a) the beam-integration method and

(b) and the percentage depth light (PDL-opt) method.with curvelet optimization

Sys. Performance: WET Accuracy

% Accuracy = $(WET_{calc} – WET_{expt}) / WET_{calc} \times 100$

Summary of relative percentage accuracies for 4 phantoms using both the reconstruction methods described in this study.

Phantoms	Beam-integration method (%)	PDL-opt method (%)
Solid water	−0.18 ± 0.35	−0.29 ± 3.11
Adipose tissue	−0.11 ± 0.51	−0.15 ± 2.64
Cortical bone	−2.94 ± 1.20	−0.75 ± 6.11
PMMA	−1.65 ± 0.35	0.36 ± 3.93

Pencil Beam Spacing

Beam integration method vs. PDL-opt method

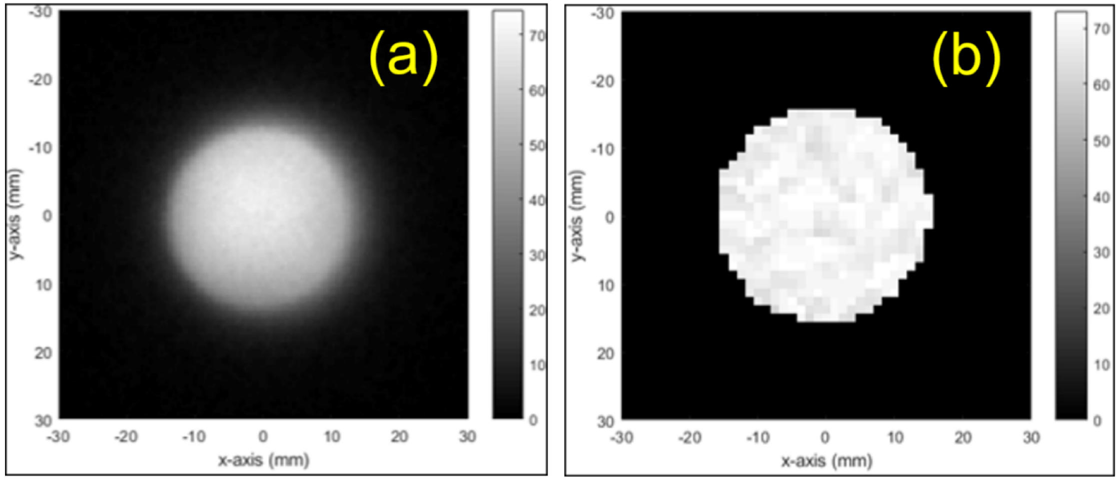

Pencil Beam grid of 2.5 mm

System Characteristics

Image uniformity = 2.6% over a 5 × 5-cm area
System stability = 0.37%
Linearity (R2) = 1

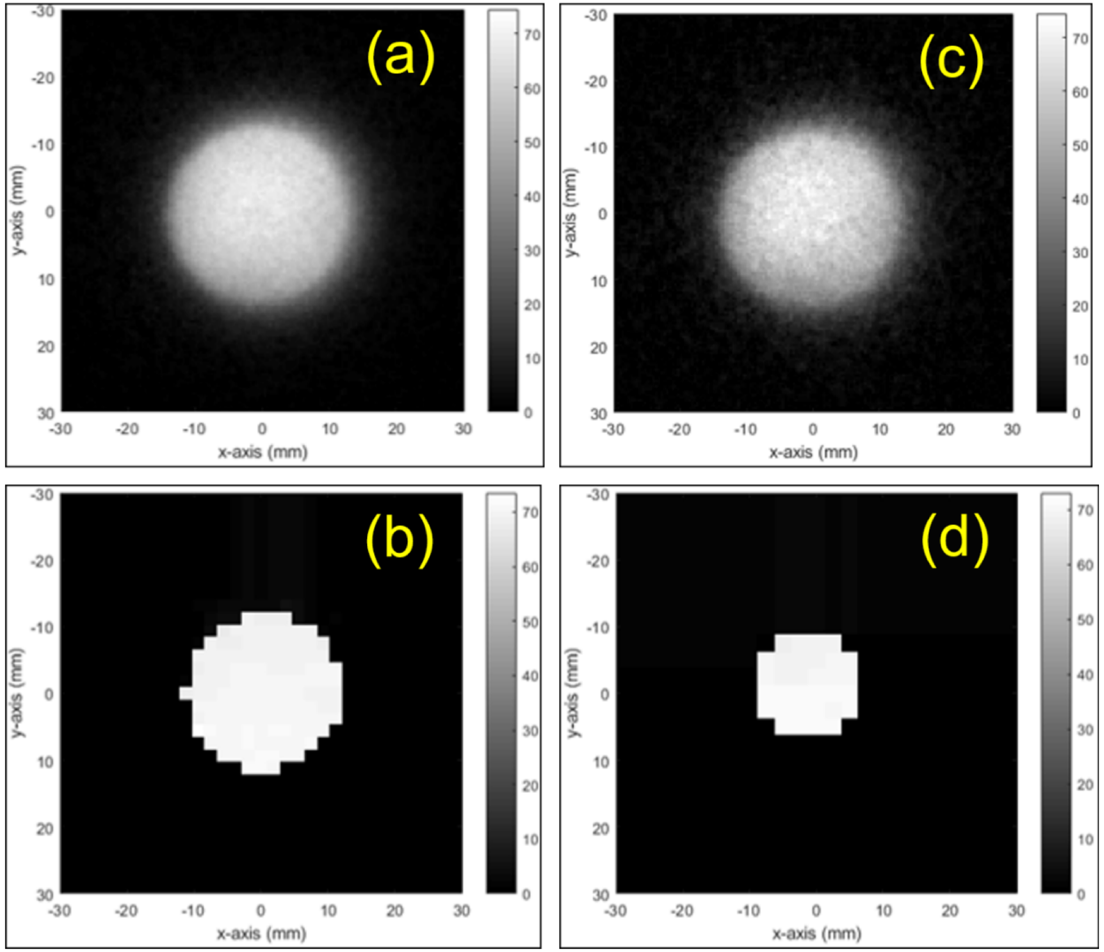

5 mm

10 mm

Resolution Pattern

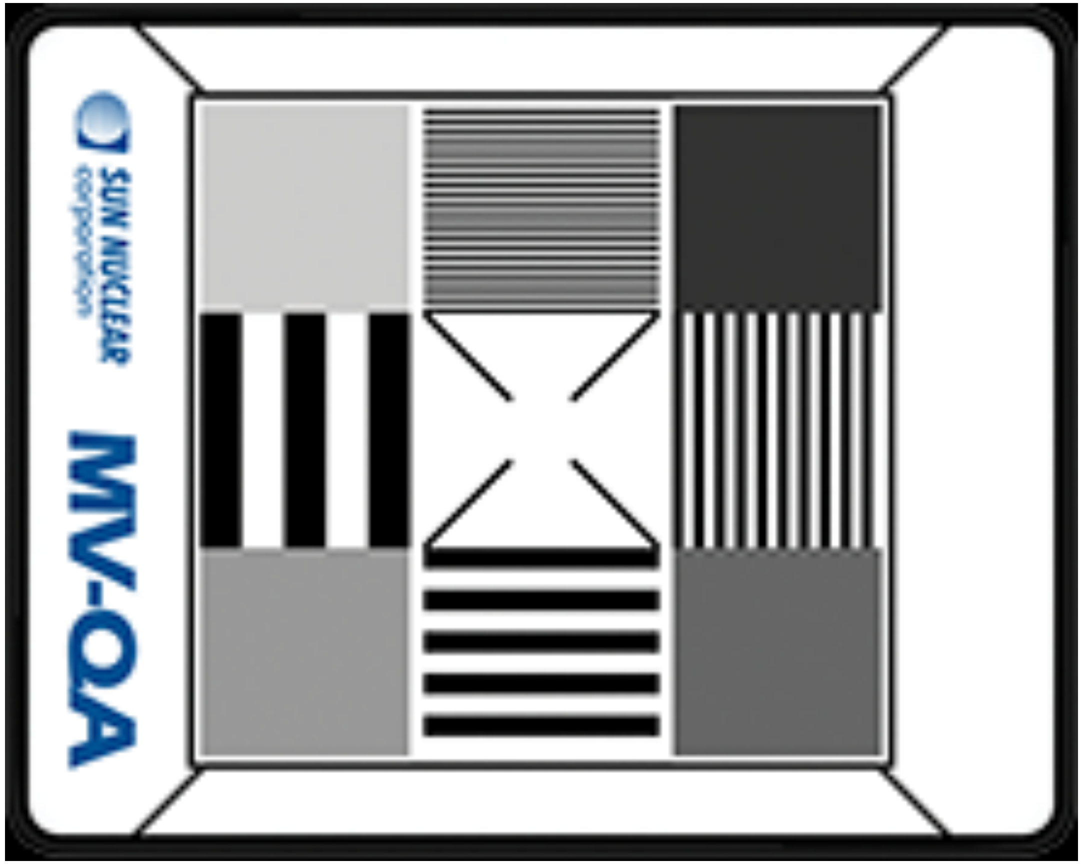

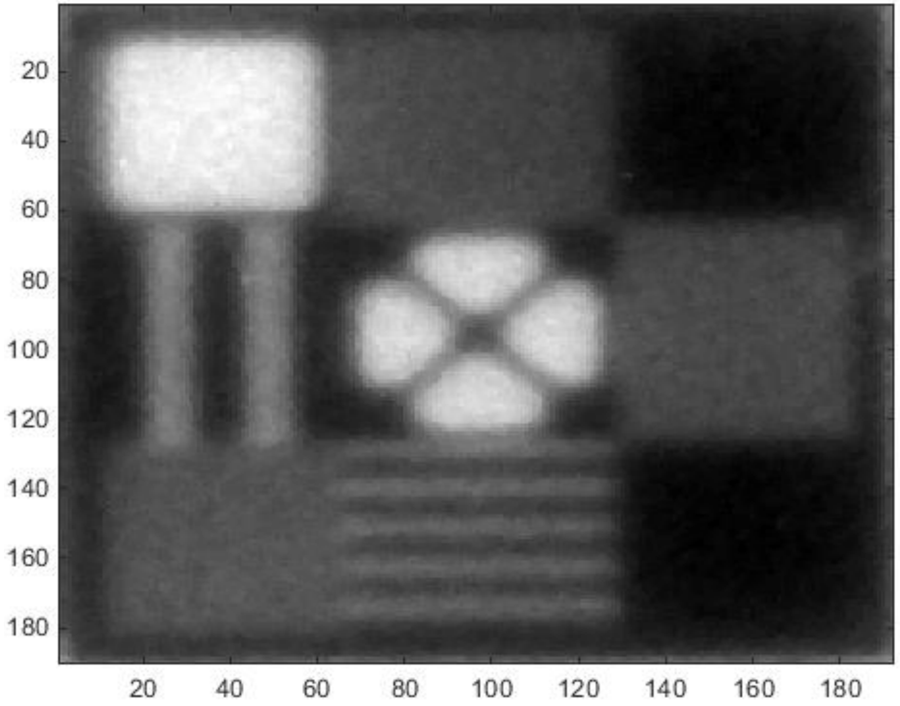

Point Spread Function

Edge of Brass Block

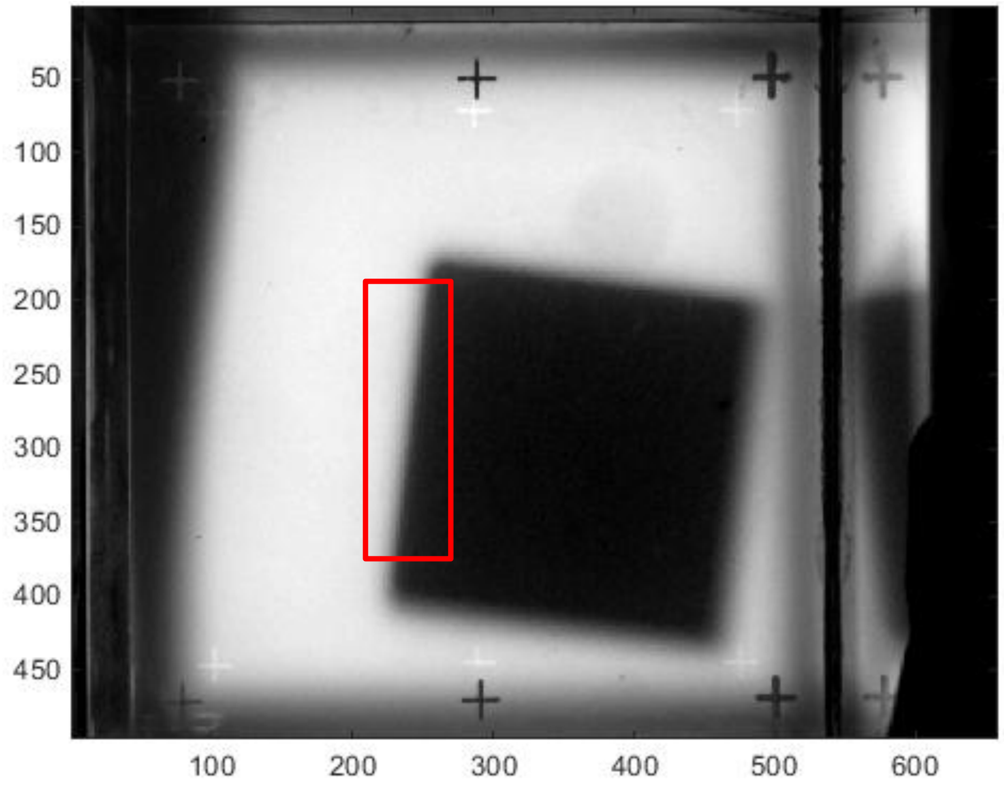

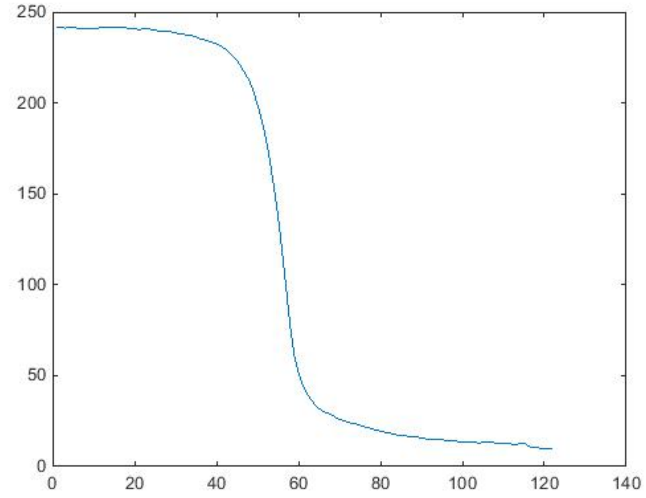

Edge spread function

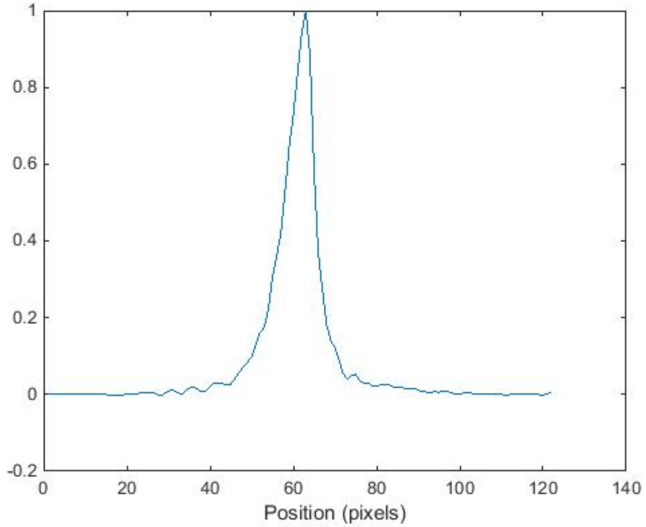

Line spread function

Courtesy of Daniel Robertson

Point Spread Function Correction

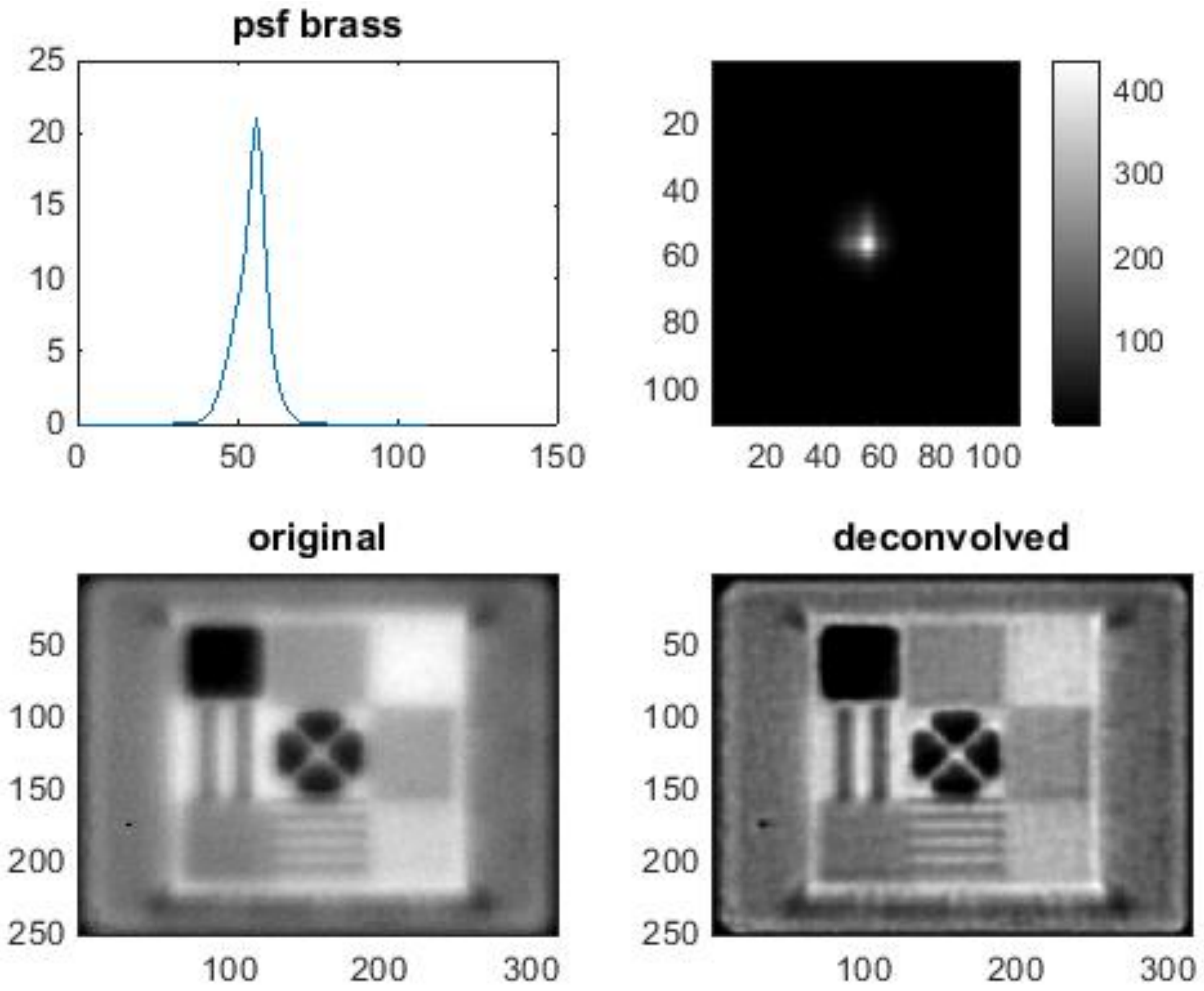

Courtesy of Daniel Robertson

Lateral Projections with Debluring

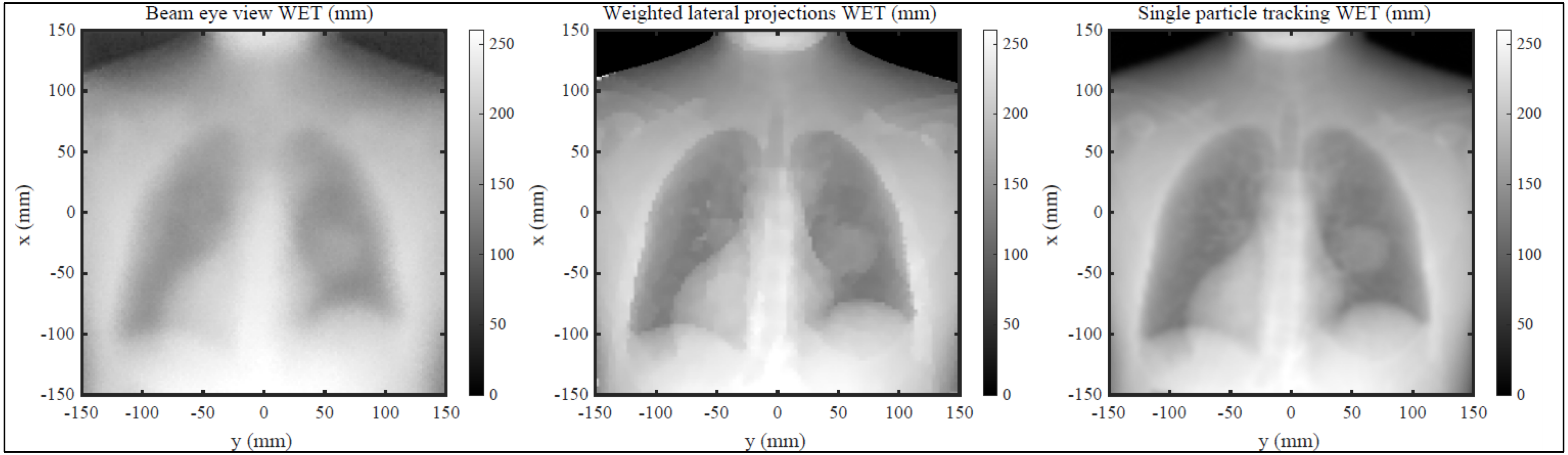

Proton radiographs of an XCAT phantom.

Left, The original beam-eye-view radiograph, where the severe blurring comes from the proton scattering from both phantom and detector.

Middle, The proton radiograph was reconstructed by deblurring the beam-eye-view radiograph using weighted lateral projections of pencil beams. Preliminary deblurring using a constant deconvolution kernel achieves a sizeable improvement in contrast.

Right, Proton radiograph reconstructed using single particle tracking method, the reference for proton imaging, included for comparison.

Courtesy of Mikaël Simard

Proton CT

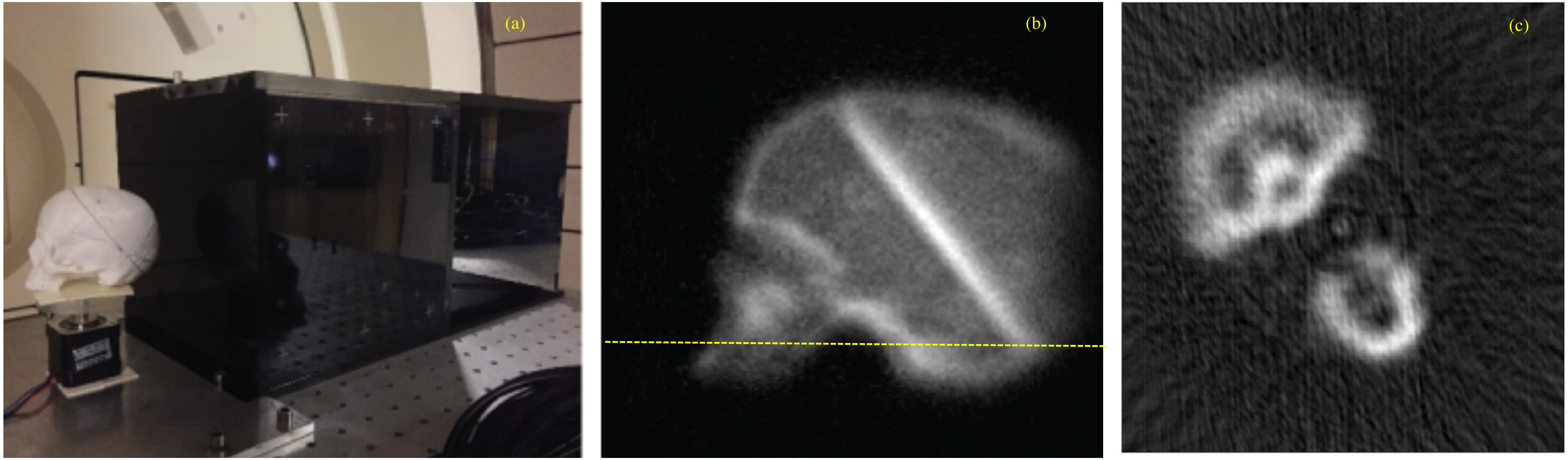

An initial proton CT image was obtained by placing the skull phantom on a rotating stage and acquiring proton radiographs using 66 projection angles. The CT was reconstructed using a filtered backprojection approach incorporating a Hamming filter.

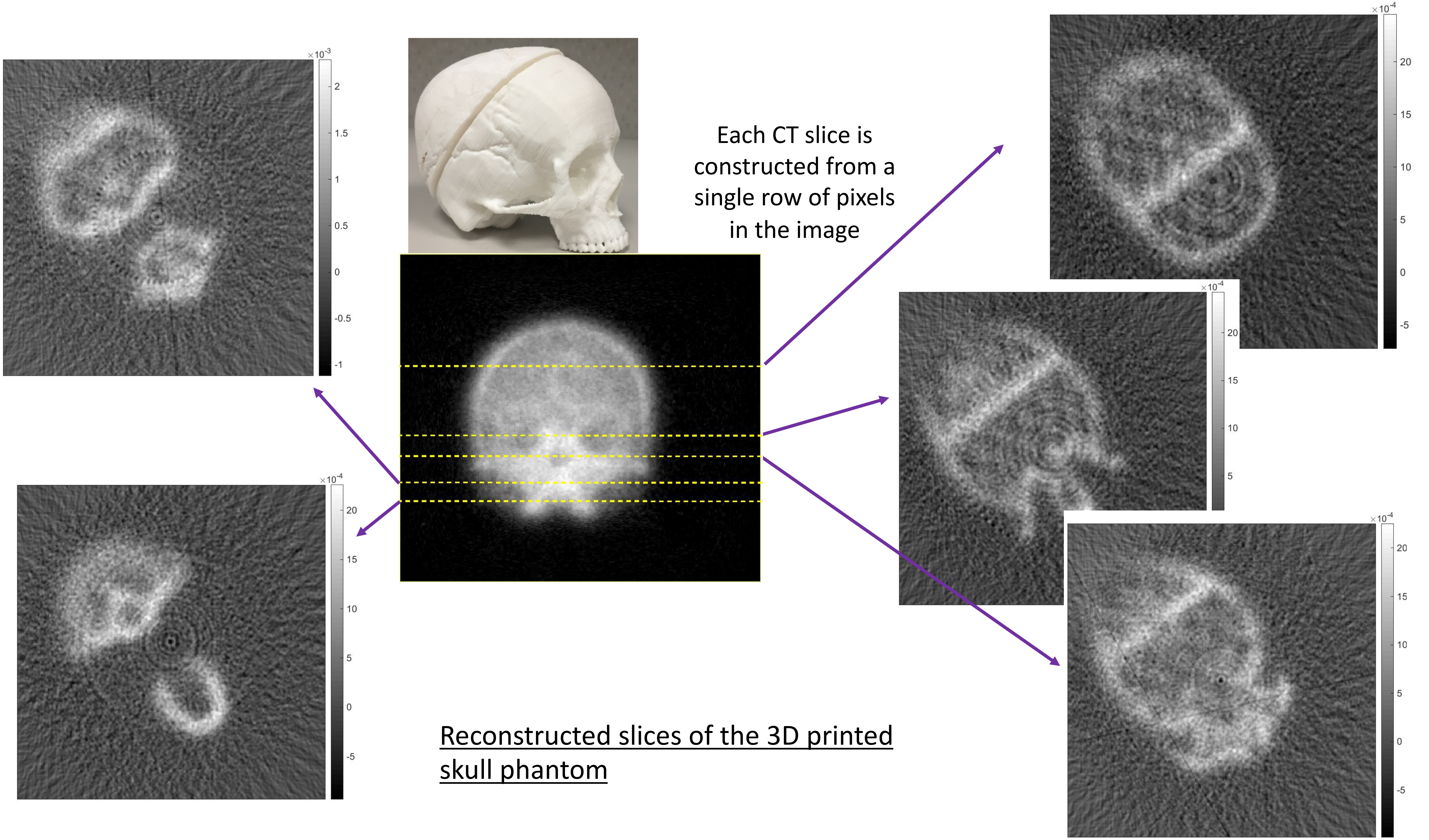

Reconstructed slices of the 3D printed skull phantom

Thank you

Acknowledgements

Daniel Robertson
Chinmay Darne
Irwin Tendler
Fahed Alsanea
Charles-Antoine Fekete
Mikaël Simard
Ryan Fullarton

THE UNIVERSITY OF TEXAS
MD Anderson ~~Cancer~~ Center
Making Cancer History®

MAYO CLINIC

UCL

Thank you

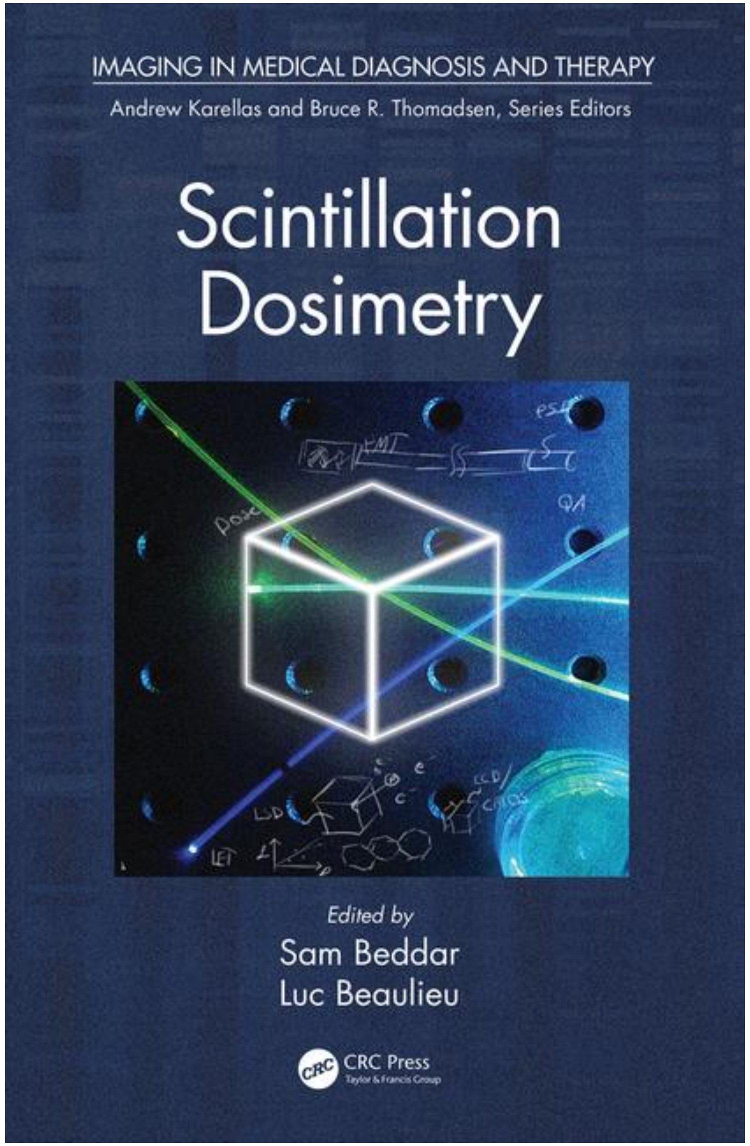

Acknowledgements

My colleagues & friends from University of Laval and Aarhus University.

My collaborators, co-authors, our students and post-doctoral fellows… and all others who have contributed to the field of scintillation dosimetry.

The Čerenkov Challenge

Stem Effect : Čerenkov

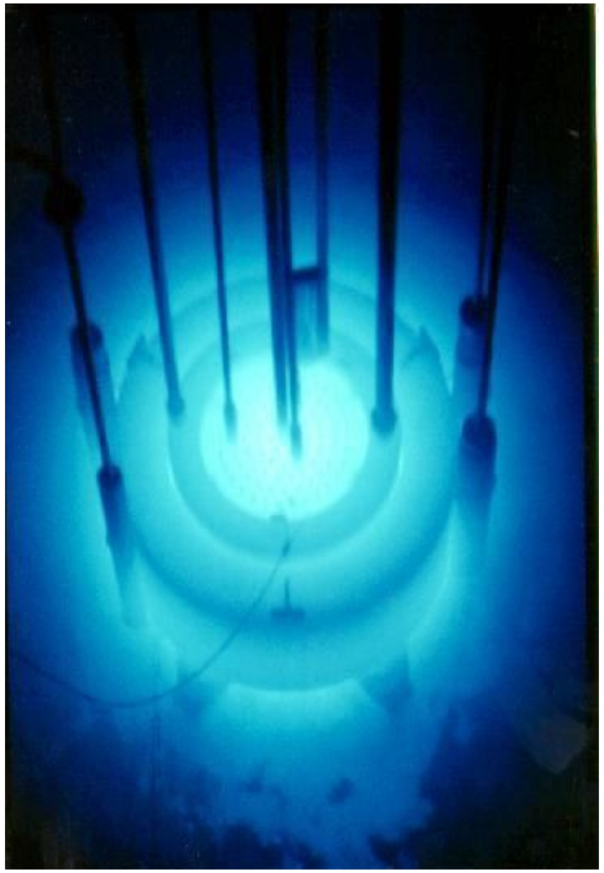

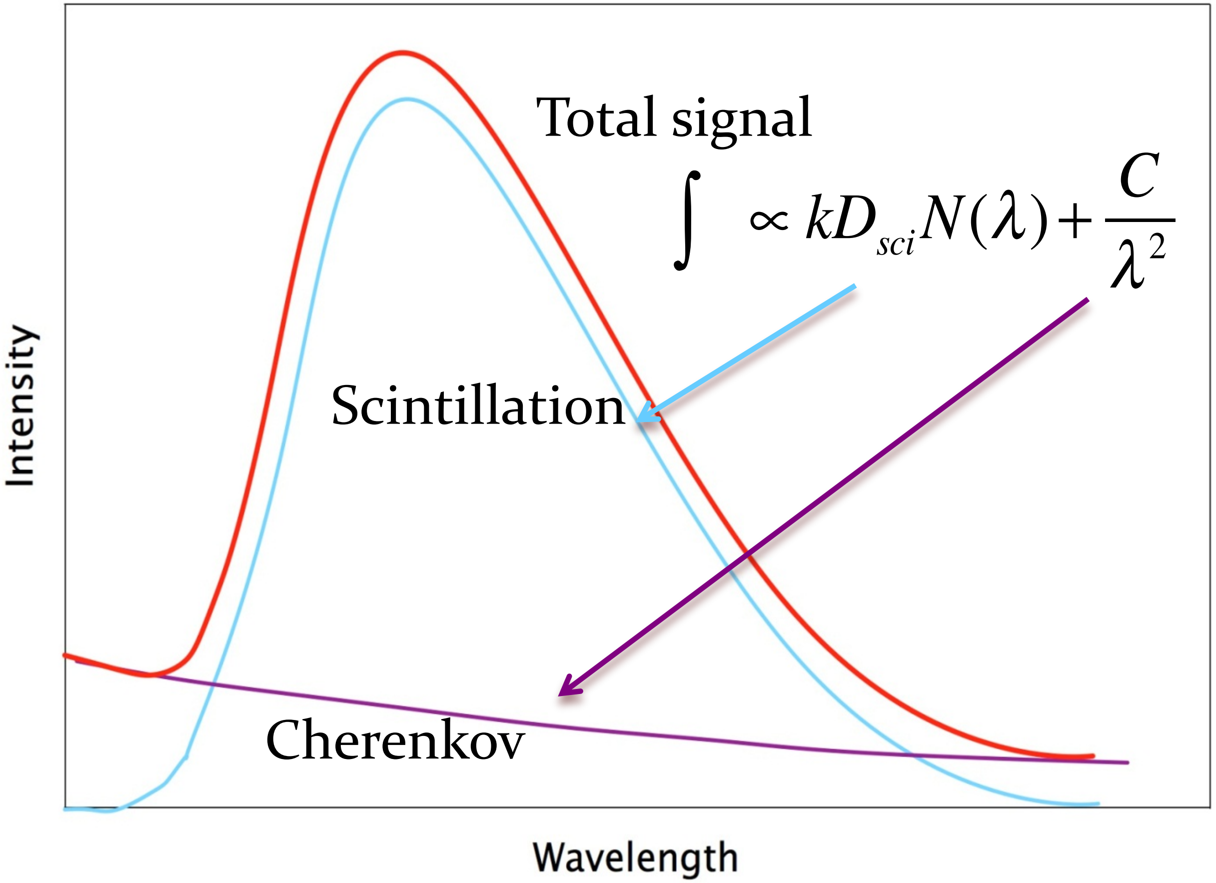

Stem Effect : Čerenkov

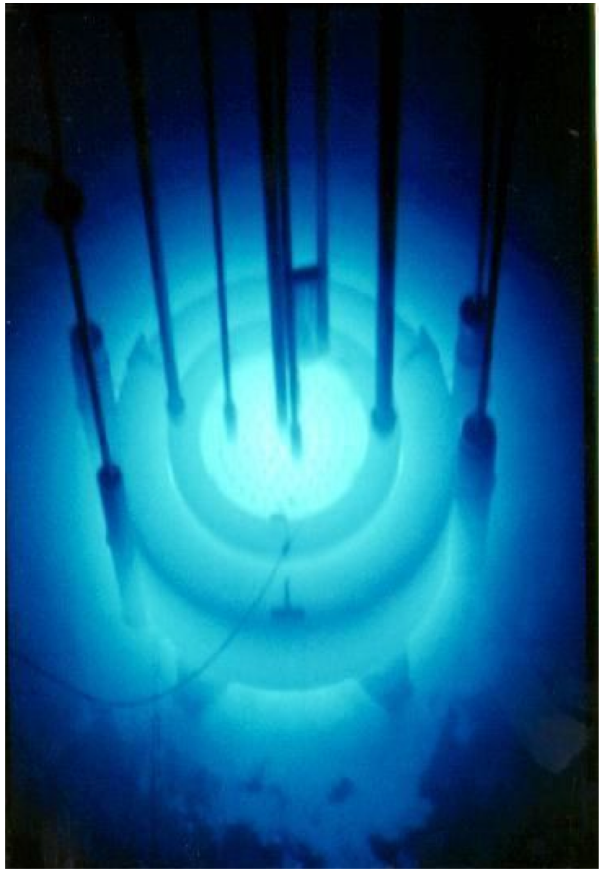

1. Background fiber substraction
2. Simple filtering
3. Timing (long decay time)
4. Chromatic removal
5. Hyperspectral decomposition
6. «Avoiding» Čerenkov generation

Beaulieu L, Goulet M, Archambault L, Beddar S. **Current status of scintillation dosimetry for megavoltage beams.** *J Phys: Conf Ser 444:* 012013, 2013.

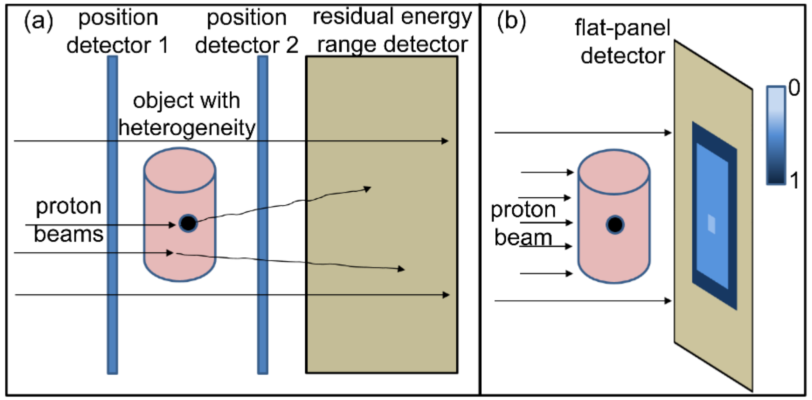

Schematics of typical (a) proton-tracking and (b) proton-integrating systems.